

Review

Emergence of Nanoplatelet Light-Emitting Diodes

Peng Xiao ¹, Junhua Huang ¹, Dong Yan ^{1,*}, Dongxiang Luo ^{2,*}, Jian Yuan ¹, Baiquan Liu ^{3,4,*} and Dong Liang ³

¹ School of Physics and Optoelectronic Engineering, Foshan University, Foshan 528000, China; xiaopeng@fosu.edu.cn (P.X.); jamha1212@163.com (J.H.); yuanjian054@163.com (J.Y.)

² School of Materials and Energy, Guangdong University of Technology, Guangzhou 510006, China

³ LUMINOUS, Center of Excellent for Semiconductor Lighting and Displays, School of Electrical and Electronic Engineering, Nanyang Technological University, Nanyang Avenue, Singapore 639798, Singapore; Dliang@scut.edu.cn

⁴ Institute of Polymer Optoelectronic Materials and Devices, State Key Laboratory of Luminescent Materials and Devices, South China University of Technology, Guangzhou 510640, China

* Correspondence: yandong2016@foxmail.com (D.Y.); luodx@gdut.edu.cn (D.L.); bqliu@ntu.edu.sg (B.L.)

Received: 6 June 2018; Accepted: 27 July 2018; Published: 8 August 2018



Abstract: Since 2014, nanoplatelet light-emitting diodes (NPL-LEDs) have been emerged as a new kind of LEDs. At first, NPL-LEDs are mainly realized by CdSe based NPLs. Since 2016, hybrid organic-inorganic perovskite NPLs are found to be effective to develop NPL-LEDs. In 2017, all-inorganic perovskite NPLs are also demonstrated for NPL-LEDs. Therefore, the development of NPL-LEDs is flourishing. In this review, the fundamental concepts of NPL-LEDs are first introduced, then the main approaches to realize NPL-LEDs are summarized and the recent progress of representative NPL-LEDs is highlighted, finally the challenges and opportunities for NPL-LEDs are presented.

Keywords: nanoplatelet; LED; CdSe; perovskite; CsPbBr₃

1. Introduction

In 1987, organic light-emitting diodes (OLEDs) have been developed, which greatly inspires researchers to take their endeavors to explore new-generation displays and solid-state lighting technologies [1]. In 1990, the first polymer LED (PLED) was demonstrated, opening the door that LEDs can be obtained by the solution-processed technology [2]. In 1994, the first colloidal quantum dot LED (QD-LED) was realized, unlocking a new technique to develop LEDs [3]. Benefiting from the understanding of OLEDs and PLEDs, the development of CdSe QD-LEDs is very fast. Currently, some QD-LED TVs are also available in the display markets. With the studying of CdSe QDs, CdSe based other nanostructures have been achieved [4–9].

Different from the semiconductor colloidal QD with a zero-dimensional (0D) structure or nanorod with a 1D structure, a semiconductor nanoplatelet (NPL) is 2D material via the management of the shape to tune the confinement of charges and as a result of its density of states [10–17]. NPLs or colloidal quantum wells have received enormous research interest since their thickness can be controlled with atomic precision and NPLs can exhibit thickness-tunable emission [18–22]. In 2006, Joo et al. reported the first CdSe nanoribbons/NPLs with a wurtzite structure via low-temperature solution-phase synthesis [23]. Since then, a large number of effective colloidal synthesis methods for NPLs have been investigated [24–26]. Compared with the conventional fabrication of inorganic quantum wells which adopts the high-vacuum technology (e.g., molecular beam epitaxy) [27], colloidal synthesis methods have greatly broadened the advantage of NPLs for practical applications (e.g., reducing the cost) [28–31].

To engineer electronic structures as well as optical characteristics, a plenty of NPLs having heterostructures have been achieved, such as core/crown NPLs, core/shell NPLs and core/crown/shell NPLs, besides core-only structures with various tuned chemical composition and vertical thickness. Besides, NPLs exhibit a number of thickness-dependent optical properties, including ultrashort radiative fluorescence lifetime, giant oscillator strength transition and narrow emission. This is because only the vertical direction exists the tight quantum confinement [32,33]. Thus, NPLs are considered to be a novel family of 2D solution-processed nanocrystals for various optoelectronic applications, including solar cells, lasers and light-emitting diodes (LEDs) [34]. For NPL-LEDs, they have great potential to lighting and displays since NPL-LEDs show a plenty of outstanding characteristics, such as excellent color purity, light weight, high efficiency as well as the compatibility to flexible substrates [35–37].

As a matter of fact, the development for NPL-LEDs lags behind other kinds of nanocrystal LEDs (e.g., QD-LEDs, nanorod LEDs, dot-in-rod LEDs). One of the main reasons is that the study of NPL-LEDs is relatively rare and only emerged in 2014 [35]. For instance, QD-LEDs can exhibit the maximum external quantum efficiency (EQE) as high as 20.5% [38]. In fact, this efficiency can be comparable with that of best OLEDs [39–48]. However, by virtue of the knowledge of other types of LEDs, it is helpful to establish high-performance NPL-LEDs. This is because the device architectures of NPL-LEDs are somewhat similar to that of other types of LEDs, particularly for the colloidal LEDs. Therefore, by enhancing the synthetic protocols for atomically flat colloidal NPLs (e.g., CdE, E = Se, S and Te) with thicknesses controlled at the atomic level, the development of NPL-LEDs is accelerating. For example, hybrid organic-inorganic ABX₃ (X is Cl[−], Br[−], or I, while A is Cs⁺ or organic groups[−]) perovskite NPLs are found to be effective to develop NPL-LEDs since 2016 [49]. Additionally, all-inorganic perovskite NPLs are also demonstrated for NPL-LEDs since 2017 [50].

In this review, we will first present fundamental concepts for NPL-LEDs. Then, we will summarize the main types of NPL-LEDs and highlighted the recent progress of representative NPL-LEDs. More specifically, we will emphasize the design strategy, NPL-LED architecture, working mechanism as well as electroluminescence (EL) procedure for representative NPL-LEDs. At last, we will introduce the challenge as well as opportunity to further enhance the performance of NPL-LEDs.

2. Fundamental Concepts of NPL-LEDs

To develop NPL-LEDs, the understanding of their basic concepts is necessary. In general, there are two different device architectures for NPL-LEDs (i.e., normal structure and inverted structure), as shown in Figure 1. However, it is deserved to note that these device structures can also be applied to other types of nanocrystal based LEDs. For the function of each layer, similar to QD-LEDs and OLEDs, the function of hole/electron injection layer is used to ensure that holes/electrons can be effectively injected into the hole/electron transport layer from the anode/cathode [51–54]. Particularly, in inverted NPL-LEDs, zinc oxide (ZnO) is demonstrated to be an efficient electron injection layer due to its high electron mobility ($\sim 1.3 \times 10^{-3} \text{ cm}^2 \text{ V}^{-1} \text{ s}^{-1}$) and suitable conduction band of 4.4 eV which well match with the work function of the commonly used cathode indium tin oxide (ITO, $\sim 4.7 \text{ eV}$) [37]. In terms of the hole/electron transport layer, they mainly function to guarantee that holes/electrons can reach the emitting layer (i.e., NPLs). Ideally, holes/electrons should be confined by the electron/hole transport layer owing to the deep HOMO (highest occupied molecular orbital) of electron transport layer/the shallow LUMO (lowest unoccupied molecular orbital) of hole transport layer [55–59]. For the emitting layer, the ligand density of NPLs have a vital influence on NPL-LEDs, since ligands have double-side effect: (i) vast ligands are necessary to give surface passivation to eliminate surface defects, resulting in high photoluminescence quantum efficiency (PLQY) and ink stability; (ii) excessive ligands can form insulating layers, preventing the charge injection in NPL-LEDs [60–64]. Hence, how to effectively control the ligand density is significant for NPL-LEDs. To date, there are some effective approaches to manage the ligands. One is the use of efficient solvents to treat the nanoparticle emitters. For example, with the hexane/ethyl acetate mixed solvents treated CsPbBr₃, the efficiency of colloidal LEDs can

be remarkably enhanced (e.g., 20 times) [60]. Another method is to exchange the long ligands with short ones, which can also improve the performance of LEDs (e.g., luminance, efficiency and stability). For example, by replacing the native octadecylphosphonic acid surface ligands with aminoethanethiol in dot-in-rod LEDs, the luminance can reach a fourfold increase [65]. Besides, the EQE has been increased from 5.1% to 5.4% and operational stability has been significantly improved [65].

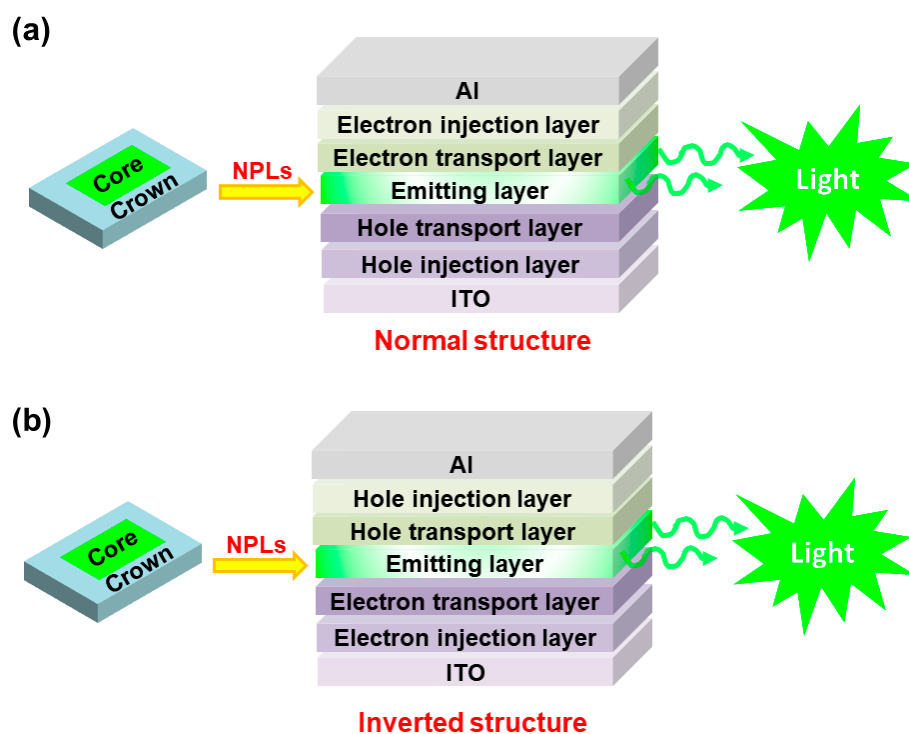


Figure 1. A schematic device architecture of NPL-LEDs. (a) Normal structure; (b) Inverted structure.

Previously, Bulović et al. have summarized that QD-LEDs can be classified into four types according to the used charge transport materials, that is, QD-LEDs using polymer charge transport layers (Type I), QD-LEDs with organic small molecule charge transport layers (Type II), QD-LEDs based on inorganic charge transport layers (Type III), QD-LEDs exploiting hybrid organic-inorganic charge transport layers (Type IV) [66–69]. In the case of NPL-LEDs, the diversity of their charge transport layers is still limited. For example, no NPL-LED with inorganic charge transport layers has been reported to date, as far as we know. Therefore, many effects of NPL-LEDs still remain unknown, indicating that efforts are urgently needed to explore the NPL-LEDs.

To boost the performance of NPL-LEDs, their emission mechanism should be well comprehended. In LEDs, EQE, power efficiency (PE) and emission color can be used to analyze the performance. For EQE, it can be described below [70–72]:

$$\text{EQE} = \eta_{out} \cdot r \cdot q \cdot \gamma \quad (1)$$

in which η_{out} represents an outcoupling factor, r represents a fraction of excitons that will radiatively decay potentially, q represents a PLQY of emitters, while γ represents a charge balance. According to the classical ray model, η_{out} is only about 0.2. Therefore, by using effective light outcoupling technologies [73–78], the EQE of NPL-LEDs can be remarkably enhanced. In addition, r as well as q would be primarily set for the used emitter. Thus, by employing efficient NPLs, high EQE can be expected. Besides, EQE is primarily sensitive to γ ($\gamma \leq 1$). Generally, a larger γ can result in more balanced charges [65]. However, charge balance is usually not good enough, since holes are

minor carriers for the inorganic material and the existed unfavorable energy barrier between nearby layers [79–85]. Hence, how to enhance the charge balance is key to NPL-LEDs.

The relation for PE and EQE is defined below, if we assumed an emission pattern is Lambertian type, [72]:

$$PE \propto \frac{EQE}{U} \quad (2)$$

in which U represents voltages. Hence, low U while high EQE is conducive to achieve high PE. By using materials with high charge mobility and/or reducing the energy barriers between the adjacent layers, low U may be obtained [86–91]. Finally, the emission color for NPL-LEDs can be generally characterized via the Commission International de L'Eclairage (CIE) chromaticity coordinates and color stability. Particularly, unlike the colloidal syntheses of spectrally narrow QDs which requires strict controls over three-dimensions, NPLs only need precise control for the thickness where quantum confinement occurs. Due to their uniform thickness, core-only and core/shell NPLs typically possess narrow full width at half maximum (FWHM) (e.g., <30 nm) [35], which is highly beneficial to the color purity.

3. Approaches to Achieve NPL-LEDs

According to the used emitting materials, NPL-LEDs can be typically categorized into three kinds, including CdSe based NPL-LEDs, hybrid perovskite NPL-LEDs and all-inorganic perovskite NPL-LEDs. In general, both normal and inverted device architectures can be used to develop these different kinds of NPL-LEDs. However, it is deserved to point out that CdSe based NPL-LEDs are currently more focused on the inverted device architectures, while perovskite NPL-LEDs are more likely to adopt the normal device architectures. Particularly, there is no inverted all-inorganic perovskite NPL-LEDs so far. These phenomena may be attributed to the fact that different NPL-LEDs may require the optimization of both material synthesis and device engineering to guarantee the high performance. In other words, design strategy, NPL-LED architecture, working mechanism and EL process for different NPL-LEDs are necessary to be clarified.

3.1. CdSe Based NPL-LEDs

3.1.1. Core/shell NPLs for LEDs

In 2014, Chen et al. reported the first colloidal NPL-LED, in which the NPL has been used the CdSe/CdZnS core/shell structure [35]. The device architecture is ITO/poly(ethylenedioxythiophene): polystyrene sulfonate (PEDOT:PSS)/poly(9-vinylcarbazole) (PVK) or poly(*N,N'*-bis(4-butylphenyl)-*N,N'*-bis(phenyl) benzidine (PTPD)/NPLs/ZnO/Al, as shown in Figure 2. To enhance the performance of NPL-LEDs, two design strategies have been used. First, exchanging the as-synthesized NPL long-chain ligands (i.e., oleic acid) to shorter ones (i.e., 3-mercaptopropionic acid), which can largely improve the charge injection. For example, the maximum EQE and luminance have been improved ~2 and ~3 times, respectively. As a result, the NPL-LED exhibits a maximum EQE of 0.63% and luminance of 4499 cd m⁻². Second, replacing the hole transport layer PVK possessing a low hole mobility of ~10⁻⁷–10⁻⁶ cm² V⁻¹ s⁻¹ with PTPD possessing a high hole mobility of ~10⁻⁵ cm² V⁻¹ s⁻¹, the driving voltage is vastly reduced. For instance, the turn on voltage has been reduced from 4.7 V to 2 V. However, the maximum EQE (0.28%) and luminance (2173 cd m⁻²) have been decreased due to this replacement, which may be attributed to the fact the charge balance in PTPD based NPL-LED is poorer than that of PVK based NPL-LED according to the Equation (1). Particularly, the narrow FWHM (25–30 nm) for the EL emission has been obtained, which was not changed by selecting LED structure or NPLs ligand during different applied voltages. Thus, these groundbreaking findings highlight the unique potential of this new class of colloidal NPLs in achieving bright, efficient and pure-color LEDs. In addition, this work demonstrated that further higher performance can depend on the enhancement of the emitting materials and the device architecture.

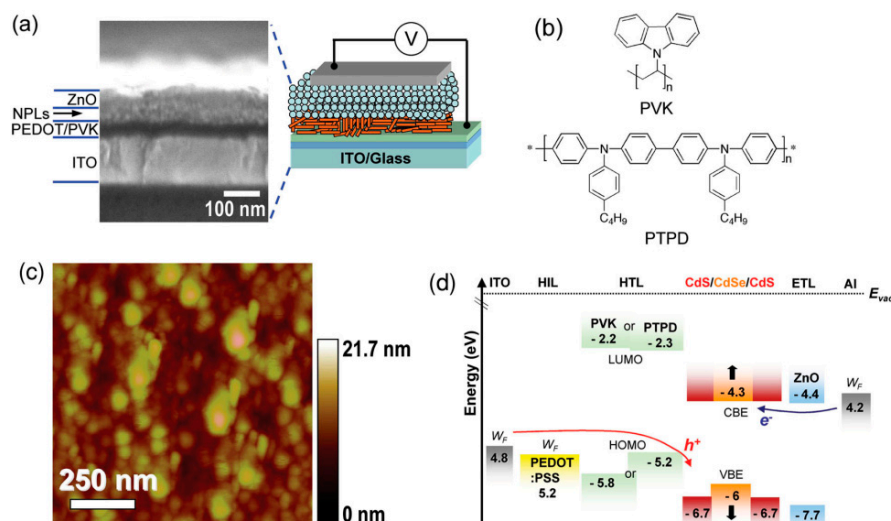


Figure 2. (a) Right: the NPL-LED device architecture. Left: cross-sectional scanning electron microscopy (SEM) for device architecture; (b) The chemical structure for hole transport materials; (c) Atomic force microscopy (AFM) for the thin film of NPLs; (d) The energy levels, VBE represents valence band edge and CBE represents conduction band edge. The black arrow indicates a shift of the band edge because of the quantum confinement. Adapted from [35], with permission from © 2013 John Wiley and Sons.

3.1.2. Core-Only NPLs for LEDs

In contrast to Chen's work [33], Vitukhnovsky et al. reported another type of NPL-LEDs [92]. First, they used bare CdSe NPLs instead of core/shell NPLs as the active emitting element. For this strategy, given that the spectrum of core-only NPLs can be much narrower compared with core/shell NPLs, this type of structure provides a great potential to develop NPL-LED having excellent color purity. Besides, the PL spectrum for core-only NPLs is generally blue-shifted than that of core/shell NPLs (e.g., CdSe NPLs range from 460 nm to 570 nm depending on the thicknesses), which is promising to develop short-wavelength LEDs. On the other hand, they implemented the CdSe core-only NPLs into a hybrid organic-inorganic device architecture of ITO/PEDOT:PSS/N, N'-bis(3-methylphenyl)-N, N'-bis(phenyl)-benzidine (TPD)/NPLs/3-(Biphenyl-4-yl)-5-(4-tert-butylphenyl)-4-phenyl-4H-1,2,4-triazole (TAZ)/Al, where TPD and TAZ are organic small-molecule hole and electron transport materials, respectively, as shown in Figure 3. For this NPL-LEDs, they considered that there were double emission mechanisms: the exciton energy transfer from organic donor molecules to NPLs as well as direct charge injection into the NPLs. As a result, the NPL-LED can exhibit a turn-on voltage of 5.5 V and an EL emission peak of 515 nm. However, the efficiencies and luminance of their NPL-LED have not been revealed, which may be attributed to the fact that the values are low.

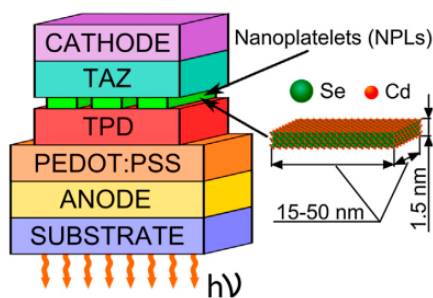


Figure 3. The NPL-LED structure. ITO, PEDOT: PSS layer, TPD, CdSe NPLs, TAZ and Al have been used as the anode, hole injection layer, hole transport layer, emitting layer and electron transport layer and cathode, respectively. Adapted from [92], with permission from © 2015 Elsevier.

3.1.3. Alloyed Core-Only NPLs for LEDs

Although previous studies have reported that colloidal NPLs could show very narrow FWHM in an order of 10 nm by elaborative syntheses [93,94], NPLs fail to provide continuous spectral tunability but rather emit at discrete wavelengths that depend strictly on atomic-layer thickness. To address this issue, Fan et al. finely tuned the emission spectra but leveraged atomic-scale thicknesses control by alloying CdSe colloidal NPLs with CdS [36]. As a result, the emissions could cover from green to blue transition regime (513–481 nm) via CdS-alloying of 6 monolayer CdSe NPLs. Then, they used these NPLs to demonstrate LEDs. The device architecture is ITO/ZnO/NPLs/4,4-*N,N*-dicarbazolebiphenyl (CBP)/MoO₃/Ag, which is an inverted structure, as shown in Figure 4. To enhance the performance of NPL-LEDs, they also examined other hole injection layer including 4,4'-cyclohexylidenebis(*N,N*-bis(4-methylphenyl)-benzenamine) (TAPC) and *N,N'*-di(1-naphthyl)-*N,N'*-diphenyl-(1,1'-biphenyl)-4,4'-diamine (NPB). After optimization, they found that the combination of hole injection layer MoO₃ and hole transport layer CBP is the best to achieve the high performance. As a consequence, the NPL-LED showing a very narrow EL spectrum of 12.5 nm, the peak brightness of ~90 cd m⁻², as well as a sub bandgap turn-on voltage of 2.1 V, has been obtained. Finally, it is deserved to note that the luminance or efficiency of both core-only and alloyed core-only NPL-LEDs is still unsatisfactory, indicating that more efforts are required to make on the developments of the core-only NPLs.

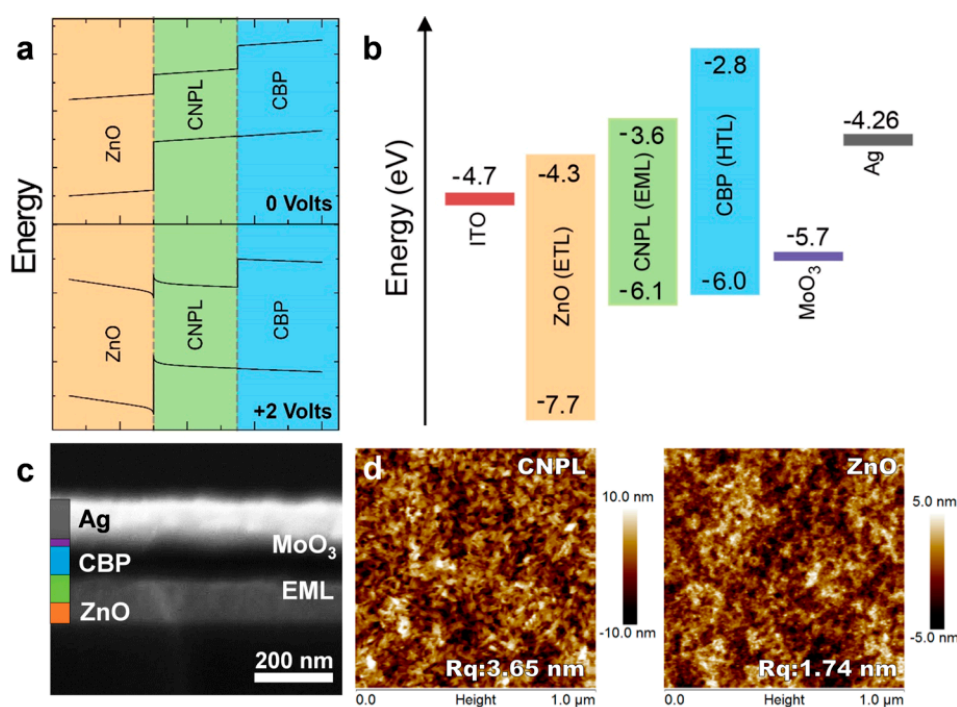


Figure 4. (a) The NPL-LED under zero-bias and forward bias near turn-on voltage (2 V), modeled using SCAPS; (b) The energy levels for NPL-LEDs; (c) Cross-sectional SEM image of the NPL-LED; (d) Left: AFM for NPLs which have been spin-coated above ZnO (the surface roughness is 3.56 nm). Right: AFM for only ZnO (the surface roughness is 1.74 nm). Adapted from [36], with permission from © 2015 American Chemical Society.

3.1.4. Core/Crown NPLs for LEDs

As mentioned above, it is not easy for semiconductor NPLs to exhibit emission wavelength tunability and only several discrete wavelengths of the NPLs are available as they are critically determined by the discrete number (2–5) of atomic layers (i.e., quantum confinement energy) [95]. Another approach for overcoming this issue can be the regulation of emission colors by using band-alignment engineering for NPLs. Unlike NPLs possessing type I heterostructures in which

the electron wave function as well as hole wave function is confined in similar place because of the wider bandgap shell or crown barriers, NPLs possessing type II band alignment (i.e., the electron as well as hole have been separated spatially) can produce different colors ranging from the visible to near-infrared region by managing the band-offset for core and shell/crown materials [96]. Besides, lowered overlap for absorptions and light spectra as well as superior emission quantum yield could be achieved for type II NPLs, endowing that them have great potential to the application of LED.

Recently, Liu et al. adopted the CdSe/CdSe_{0.8}Te_{0.2} core/crown type II NPLs as the emitter for LEDs [37]. The device architecture is ITO/ZnO/NPLs/TCTA/TPD/MoO₃/Al, where TCTA/TPD is a dual hole transport layer, as depicted in Figure 5. For ensuring excellent performance, they used an efficient NPLs with PLQY of 85%. Another key for their high performance is the exploitation of the dual hole transport layer, which is much better than the single hole transport layer CBP or TPD. This is because (i) more excitons could be formed when more holes could meet electrons in TCTA/TPD based NPL-LED, since TCTA is hole-dominating and has a higher LUMO to confine the electrons in NPLs [97]; (ii) more holes can be injected into the NPLs in TCTA/TPD based NPL-LED, because TCTA/TPD can reduce the hole barrier due to the step-wise HOMO [98]; (iii) better charge balance is achieved in TCTA/TPD based NPL-LED, considering that the electron is readily injected to NPLs due to high electron mobility for ZnO as well as low LUMO barrier for NPLs and ZnO [38]; (iv) the dual hole transport layer can be helpful to remain charge neutrality for NPLs and maintain the good emissive characteristics [9]. As a result, the NPL-LED achieved the extremely low turn-on voltage, high brightness, high EQE and PE of 1.9 V, 34,520 cd m⁻², 3.57% and 9.44 lm W⁻¹, respectively. Also, this work demonstrated that more attentions are necessary to be paid on the improvement of device architectures, if elegant NPLs have been obtained.

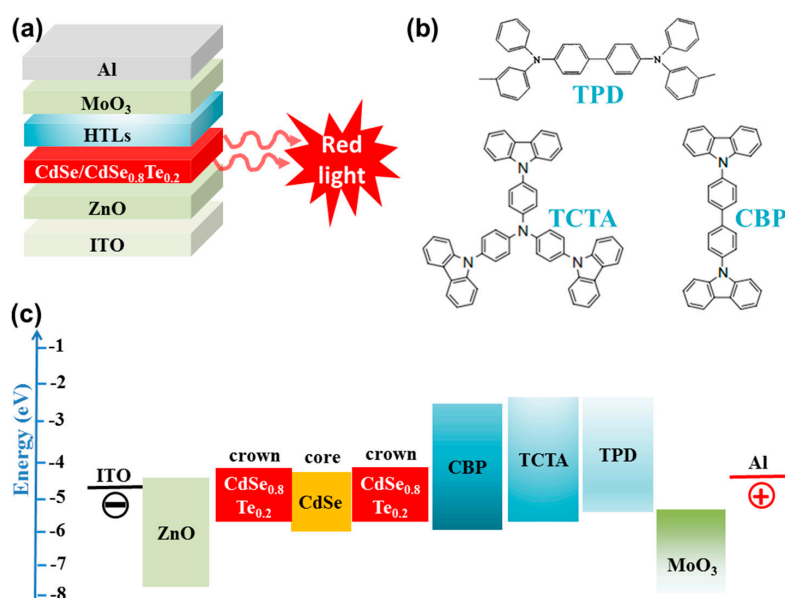


Figure 5. (a) The NPL-LED structures; (b) The molecular structures for hole transport materials; (c) The proposed energy levels for NPL-LEDs. Adapted from [37], with permission from © 2018 Elsevier.

3.2. Hybrid Organic-Inorganic Perovskite NPL-LEDs

Over the past few years, earth-abundant lead halide perovskites have emerged as a novel class of optoelectronic materials for applications including solar cells, lasers and photodetectors due to the outstanding characteristics (e.g., good carrier-transporting capability, size-tunable optical bandgap and narrow emission) [99–105]. Besides, the outstanding characteristics have endowed the perovskite materials appropriate for LEDs [106]. After the development of bright organic-inorganic hybrid CH₃NH₃PbBr₃ perovskite LED in 2014 [107], both academic and industrial researchers

have paid a great deal of attention to this new kind of LEDs [108–110]. To date, perovskite LEDs have been demonstrated to exhibit bright luminescence, excellent color purity with narrow EL emission, broadband color tenability and high charge mobility [111–113]. Besides, the highest EQE of organic-inorganic hybrid perovskite LEDs could be >11% [114].

For perovskite LEDs, although a large number of endeavors have been taken on 3D nanocubes based devices, the attention for perovskite NPL-LEDs which are based on 2D nanoplatelets is rapidly increasing. Different from 3D perovskites, the cubic symmetry in 2D perovskites has been broken and metal halide layer for original 3D structures could be divided to the $\langle 110 \rangle$ or $\langle 001 \rangle$ oriented slice. For broken symmetry, it can reduce forbidden electronic transitions as well as enhance the PLQY [115–117]. Thus, due to the improved interaction between holes and electrons via the self-organized quantum-well structure, strong confining excitons showing binding energy above 200 meV is yielded, which is helpful for LEDs [118]. Besides, the 2D perovskite may exhibit broader bandgaps as well as narrower emissions than the 3D ones due to the introduction of quantum confinement effect [119,120]. Following this logic, Liang et al. used 2D perovskites 2-phenylethylammonium lead bromide ((PEA)₂PbBr₄) to be emitter to realize violet perovskite LEDs, where the organic cation PEA (also called phenethylammonium) is C₆H₅CH₂CH₂NH₃⁺ [49]. In general, layered 2D organolead halide perovskites can be described by the formula (RNH₃)₂PbX₄, where R is an aryl or alkyl substituent and X is a halogen [121–123]. The device structure is ITO/PEDOT:PSS (30 nm)/(PEA)₂PbBr₄/1,3,5-tris(1-phenyl-1H-benzo[d]imidazol-2-yl)benzene (TPBi, 35 nm)/Ca (25 nm)/Al (100 nm), as shown in Figure 6. The LED displays an EL emission peak of 410 nm and FWHM of 14 nm, as well as an EQE of 0.002%. To enhance the efficiency, they have converted the as-deposited polycrystalline (PEA)₂PbBr₄ thin films into high-quality micrometer-sized single-crystal NPLs by the dimethylformamide solvent vapor annealing. As a result, an EQE of 0.04% is obtained. However, from the EL emission (Figure 6C), it can be seen that the parasitic emission of TPBi (375 nm) cannot be avoided, which may be attributed to the discontinuous surface coverage by NPL layer.

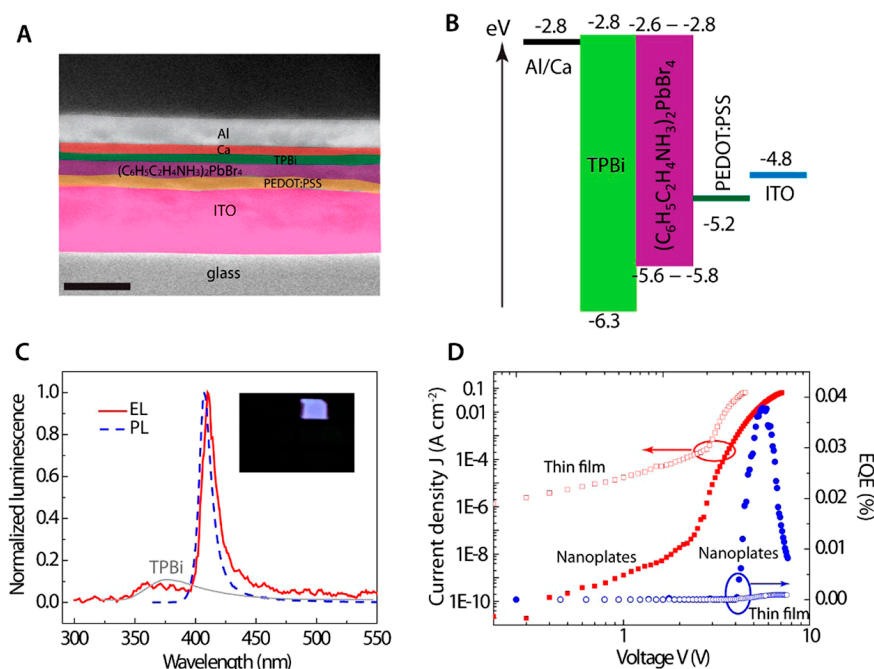


Figure 6. (A) The SEM for LEDs (scale bar: 200 nm); (B) The energy levels of LEDs; (C) Normalized luminescence of the LED using (PEA)₂PbBr₄ NPLs achieved from dimethylformamide vapor annealing at 6 V. EL and PL emission peaks are located at 410 and 407 nm, respectively. Inset: a picture for violet light from the (PEA)₂PbBr₄ LED; (D) Current-voltage dependence (red symbols) and EQE (blue symbols) for LEDs fabricated with the (PEA)₂PbBr₄ thin film (open symbols) and NPLs (solid symbols). Adapted from [49], with permission from © 2016 American Chemical Society.

To enhance the performance of hybrid perovskite NPL-LEDs, perovskites with high crystallinity as well as high PLQY are crucial [124–126]. For this purpose, Ling et al. fabricated bright hybrid perovskite NPL-LEDs with maximum luminance of $10,590 \text{ cd m}^{-2}$ (emission peak at 530 nm), a PE of 1.0 lm W^{-1} and EQE of 0.48% [127]. The device architecture is ITO/PEDOT:PSS/PVK: 2-(4-biphenyl)-5-phenyl-1,3,4-oxadiazole (PBD): $\text{CH}_3\text{NH}_3\text{PbBr}_3$ /bathocuproine (BCP, 50 nm)/LiF (1 nm)/Al (150 nm), as shown in Figure 7. By utilizing well-known precursors as well as organic solvent, high performance crystalline $\text{CH}_3\text{NH}_3\text{PbBr}_3$ (MAPbBr₃) NPLs (i.e., PLQY = 85%) have been produced, which is crucial to the LED. Besides, by using bipolar PVK:PBD in the emitting layer, charge balance has been optimized, which is also responsible for high performance. For example, without this bipolar host, the LED only exhibits EQE of 0.038% and luminance of 1113 cd m^{-2} . Furthermore, their perovskite-NPLs materials is very stable. For instance, with humidity (~55%) for at least one week, the perovskites endow fabricating perovskite LEDs without using the inert-gas glovebox.

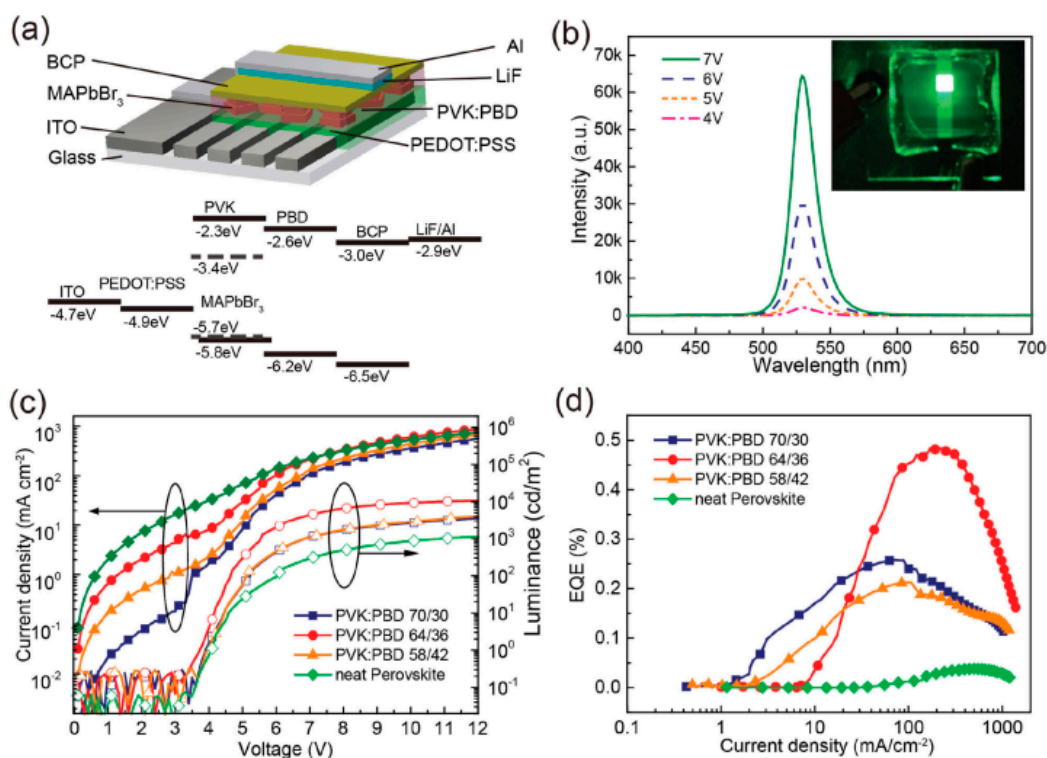


Figure 7. (a) Device architecture for a LED and the energy levels; (b) The EL spectrum of the standard LED using PVK: PBD weight ratio of 64/36 at 4–7 V. Inset: a picture for the perovskite LED under 7 V; (c) Current-voltage and luminance-voltage properties of the control LED (neat perovskites without PVK:PBD) and LEDs using PVK:PBD (ratio of 70:30, 64:36 and 58:42) layer; (d) EQE-current density of LEDs. Adapted from [127], with permission from © 2015 John Wiley and Sons.

Aside from methylammonium lead bromide (MAPbBr₃), formamidinium lead bromide (FAPbBr₃) is another type of hybrid perovskite materials for LEDs. Similar to MAPbBr₃, 2D FAPbBr₃ NPLs can be very efficient emitters. Recently, with about 7–10 unit cells colloidal FAPbBr₃ NPLs, Kumar et al. have reported a pure green LED [128]. The exciton-binding energy as high as 162 meV for 2D FAPbBr₃ perovskites via the dielectric quantum well engineering. As a consequence, the PLQY as high as 92% for thin film. Then, by optimizing the device architecture (e.g., both the hole and electron transport), the champion structure of ITO/PEDOT:PSS/poly-TPD/PMMA:FAPbBr₃/3TPYMB/LiF/Al is obtained, as displayed in Figure 8. Thus, the LED exhibits the peak current efficiency as high as 13.02 cd A^{-1} . Besides, the FWHM of 22.8 nm and an EL peak located at 529 nm could be achieved, leading to a CIE 1931 coordinates of (0.168, 0.773). Hence, their LED possesses a wide color gamut,

which can cover 97% of the Rec. 2020 standard in the CIE 1931 color space. Compared with the LED without PMMA, the efficiency of LED using FAPbBr₃-PMMA complex significantly improves (~3 times), which can be attributed to dielectric confinement effect and formation of a smoother emitting layer. In addition, the superior device performance can be attributed to the effective exciton recombination as well as the balanced charge, which can be explained as follows. First, the cascade carrier injection is achieved by the deep LUMO of 3TPYMB (3.3 eV) as well as shallow HOMO of poly-TPD (5.4 eV). Second, 3TPYMB and poly-TPD possess comparable carrier mobilities. Besides, the deep HOMO 3TPYMB (6.8 eV) together with the shallow LUMO of poly-TPD (2.0 eV) can form an effective carrier confinement.

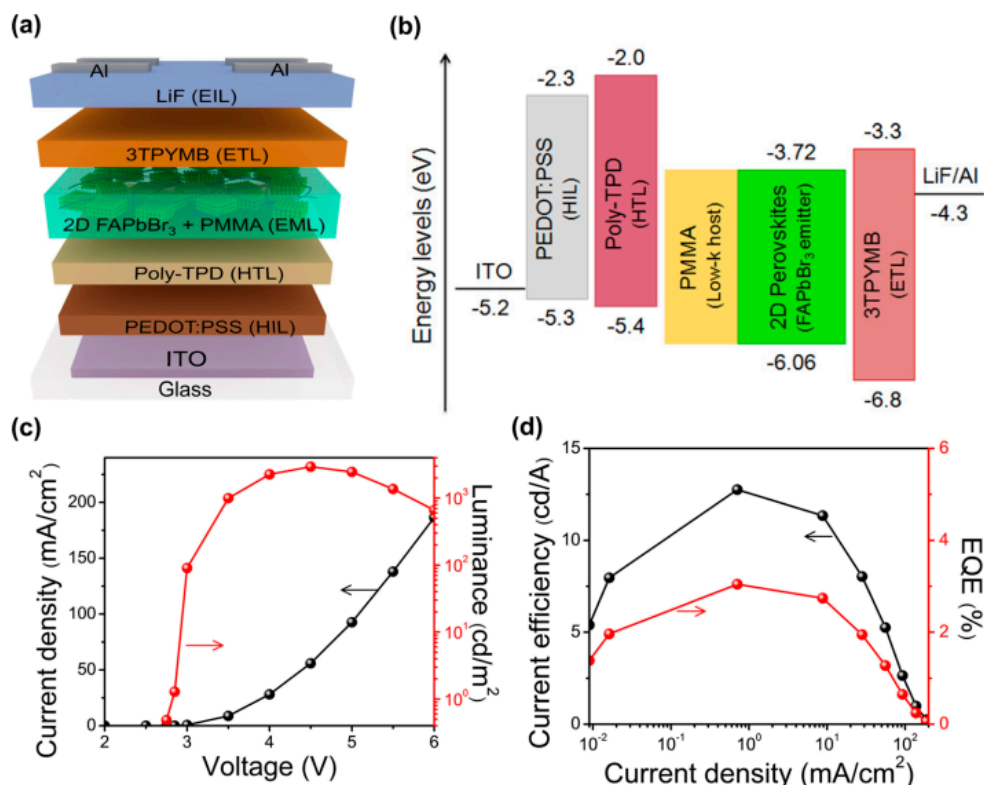


Figure 8. Properties for LEDs based on 2D FAPbBr₃ perovskites. (a) The LED structure; (b) Energy levels of materials; (c) Current density as well as luminance; (d) Current efficiency as well as EQE. Adapted from [128], with permission from © 2017 American Chemical Society.

3.3. All-Inorganic Perovskite NPL-LEDs

For hybrid organic-inorganic perovskite materials, they have been well demonstrated to develop high-efficiency LEDs. However, this kind of material usually have a stability problem. As an alternative, all-inorganic perovskites CsPbX₃ (X = I, Br and Cl or mixed halide) show better thermal stabilities, which may overcome the notorious stability issue [129–131]. In addition, since all-inorganic perovskites can show narrow emission (e.g., FWHM < 20 nm) and excellent PLQY (e.g., ~100% in solution), they have triggered great interest to develop LEDs [132–136]. After the first LED with all-inorganic perovskites developed in 2015 [137], many methods were used to enhance the performance of this kind of LEDs based on 3D nanocubes [138–140]. For 2D all-inorganic perovskite NPLs, Bekenstein et al. first reported CsPbX₃ NPLs showing the 1–5 unit cells thickness in 2015 [141]. Since then, many efforts have been focused on synthesizing precisely tunable as well as uniform CsPbX₃ NPLs [142–145]. Currently, colloidal NPLs of perovskite metal halides have been found to be a significant family of materials for LEDs, which enriches the diversity of semiconducting nanomaterials and provide a platform for exploring new optoelectronic properties of 2D semiconducting materials.

In 2016, Zhang et al. used the mixture of 2D CsPb₂Br₅ and 3D CsPbBr₃ as the emitter to realize perovskite LEDs, exhibiting an EQE of 2.21%, a current efficiency of 8.98 cd A⁻¹ and a maximum luminance of 3853 cd m⁻² [146]. Hence, this dual-phase all-inorganic composite CsPbBr₃-CsPb₂Br₅ composite nanocrystals present a new route of perovskite material for light emission applications. Particularly, the parasite of secondary phase CsPb₂Br₅ nanoparticles on the cubic CsPbBr₃ nanocrystals can (i) improve current efficiency by lowering diffusion length of excitons; (ii) reduce the trap density in the bandgap; (iii) enhance the ionic conductivity by lowering the barrier against the electronic and ionic transport; (iv) enhance emission lifetime by reducing non-radiative energy transfer to trap states by controlling trap density, which is a key to the high performance. However, detailed EL as well as optical properties for single-component CsPb₂Br₅ film was not reported [147–150].

In 2017, Qin et al. studied the optical, structural as well as EL properties of pure CsPb₂Br₅ films [50]. With the centrifugal coating technology, the CsPb₂Br₅ film has PLQY of ~35%, which is highly desired to develop NPL-LEDs. By using this CsPb₂Br₅ NPL, LEDs were fabricated with a structure of ITO (100 nm)/PEDOT:PSS (30 nm)/CsPb₂Br₅ (30 nm)/TPBi (40 nm)/LiF (0.8 nm)/Al (100 nm), as shown in Figure 9. The NPL-LED exhibits a bright-green emission showing the peak at 520 nm as well as the CIE coordinates of (0.08, 0.75). Besides, the NPL-LED shows a maximum luminance of 7317 cd m⁻², turn-on voltage of 3.8 V, EQE of 1.1%, as well as good stability. Furthermore, by exchanging halogen Br with I in CsPb₂Br₅, a red emission has been obtained by CsPb₂I₅. The CsPb₂I₅ films have an emission peak wavelength of 685 nm, an optical bandgap of 1.75 eV and a PLQY of ~15%. With a same device architecture except for the emitter, the red NPL-LED has the peak EQE of 0.14%.

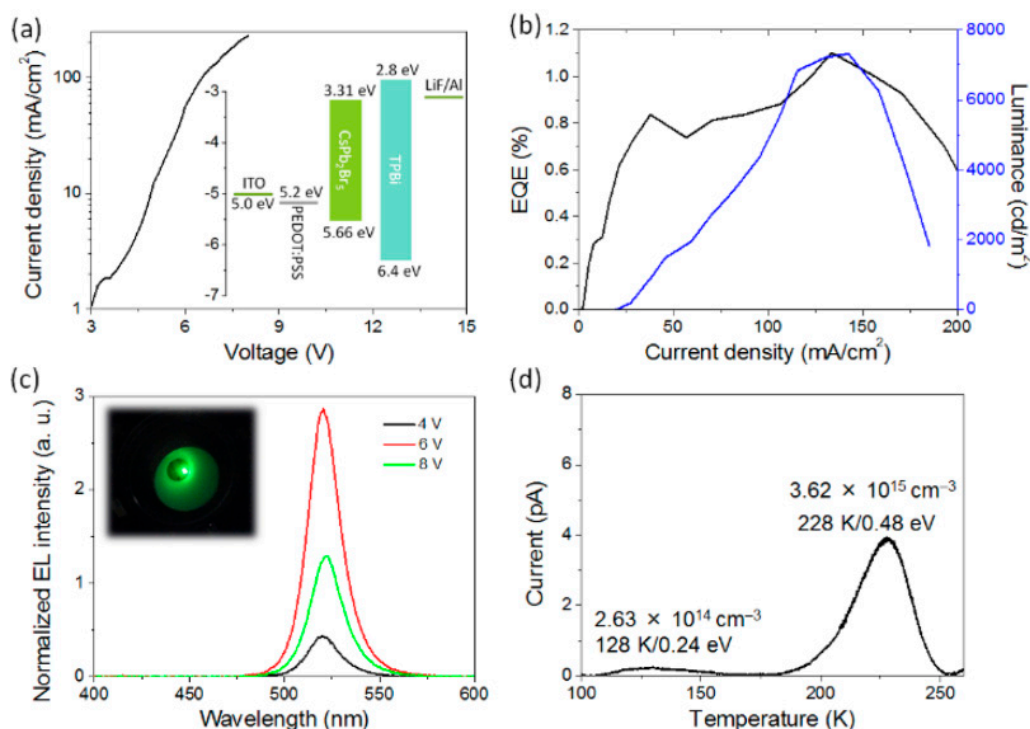


Figure 9. (a) Current density-voltage properties. Inset: a diagram of energy levels; (b) EQE and luminance as a function of current density; (c) EL spectra measured at various voltages. Inset: a picture of LED at 10 mA cm⁻²; (d) Thermally stimulated current profile with calculated values of carrier trap depth and concentration for CsPb₂Br₅ perovskite LEDs. Adapted from [50], with permission from © 2017 American Chemical Society.

According to the EL emissions, CsPbCl₃, CsPbBr₃ and CsPbI₃ can furnish red green and blue color, respectively. However, when various nanocrystal CsPbX₃ have been utilized together as emitters in LEDs, the fast anion exchange can occur [151,152]. As a solution, 2D CsPbX₃ nanocrystals with

precisely tunable thickness are promising to optoelectronic applications due to the merits, particularly for their quantum confinement effect [153,154]. Toward this end, Yang et al. demonstrated that ultrathin CsPbBr₃ NPLs having precisely tunable dimensions could be achieved in a large scale via a simple one-pot method and could be utilized to be the emitting layer of blue LEDs [155]. The device architecture is ITO/PEDOT:PSS/poly-TPD/CsPbBr₃ NPLs/TPBi/LiF/Al, as shown in Figure 10. For the CsPbBr₃ NPLs, their thickness can be precisely varied in a monolayer level by controlling the reaction kinetics. Besides, due to the high uniformity, no purification is required. In addition, through changing the reaction time, edge length could be adjusted broadly. As a result, the NPL-LED can exhibit an EQE of ~0.1% and a maximum luminance of 25 cd m⁻². After this report, blue, green and red colors have been realized in all-inorganic perovskite NPL-LEDs. Finally, it is believed that the performance (e.g., efficiency, luminance) of perovskite NPL-LEDs can be much higher via the enhancement of both NPL emitters and LED architectures.

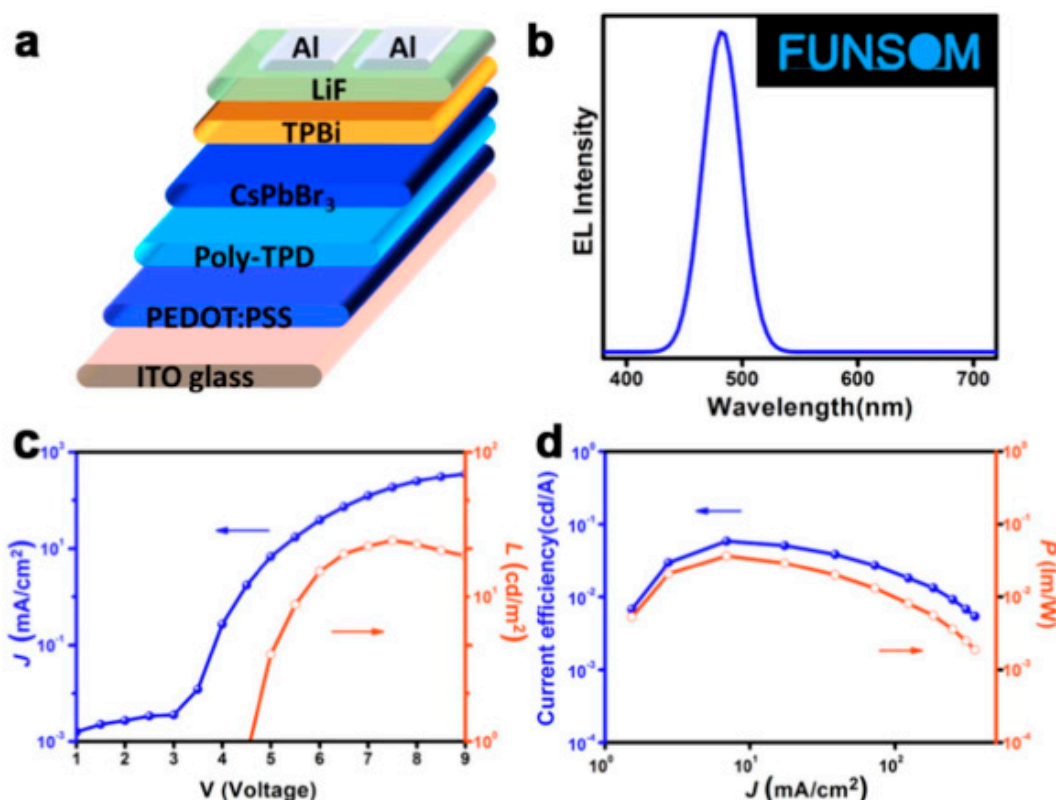


Figure 10. (a) The LED structure; (b) EL spectra. Inset: a picture of the operated LED; (c) Current density (J)-Voltage (V)-Luminance (L) curves; (d) Current efficiency- J -Power efficiency (P) curves. Adapted from [155], with permission from © 2018 Elsevier.

4. Summary and Outlook

As a new class of optoelectronic materials, NPLs exhibit a number of advantages, which is promising to establish high-performance LEDs. Over the past 4 years, the performance of NPL-LEDs has been step-by-step enhanced. Although NPL-LEDs still lag behind state-of-the-art QD-LEDs and OLEDs, currently, it is believed that NPL-LEDs can be comparable to their counterparts in the foreseeable future. Herein, the development of various NPL-LEDs has been presented. Particularly, we have highlighted recent development of CdSe based NPL-LEDs (including core/shell, core-only, alloyed core-only and core/crown NPLs), hybrid perovskite NPL-LEDs and all-inorganic perovskite NPL-LEDs. The detailed performances of representative NPL-LEDs are shown in Table 1.

Table 1. Summary of the performances of representative NPL-LEDs.

Devices	V_{on}^a (V)	EQE_{max}^b (%)	CE_{max}^c ($cd A^{-1}$)	PE_{max}^d ($lm W^{-1}$)	L_{max}^e ($cd m^{-2}$)	λ_{max}^f (nm)	CIE g
Ref. [35] ^h	4.7	0.63	-	-	4499	~645	(0.73, 0.29)
Ref. [36] ^h	2.1	-	-	-	~90	520	-
Ref. [37] ^h	1.9	3.57	-	9.44	34,520	599	(0.61, 0.38)
Ref. [92] ^h	5.5	-	-	-	-	515	-
Ref. [49] ⁱ	-	0.04	-	-	-	410	-
Ref. [127] ⁱ	3.8	0.48	-	1.0	10,590	530	-
Ref. [128] ⁱ	2.75	3.4	13.02	13.36	2939	529	(0.168, 0.773)
Ref. [50] ^j	3.8	1.1	-	-	7317	520	(0.08, 0.75)
Ref. [50] ^j	4.0	0.14	-	-	-	693	(0.69, 0.26)
Ref. [155] ^j	-	0.1	-	-	25	480	-

^a Turn-on voltage; ^b Maximum EQE; ^c Maximum current efficiency; ^d Maximum PE; ^e Maximum luminance; ^f The EL emission peak; ^g The CIE coordinates; ^h CdSe based NPL-LEDs; ⁱ Hybrid perovskite NPL-LEDs; ^j All-inorganic perovskite NPL-LEDs.

To achieve higher performance, there are still many challenges before NPL-LEDs can be as good as QD-LEDs and OLEDs, such as the efficiency and lifetime. In the case of efficiency, there is much room for EQE of NPL-LEDs to the theoretical limit of 20% (assuming the outcoupling factor is 0.2) [156]. According to Equation (1), the use of efficient NPLs, careful manipulation of charge distribution and the introduction of outcoupling technique are helpful to boost the EQE [157–162]. In addition, the introduction of tandem architecture is beneficial to the efficiency [163–167], although no tandem NPL-LED has been developed. Besides, the efficiency roll-off of NPL-LEDs is unsatisfactory. As a consequence, the efficiency at high luminances is not good enough. Hence, charge balance, energy barrier as well as material selection are needed to be managed [168–172]. In terms of the lifetime, only negligible attention was paid to NPL-LEDs. For practical applications, long lifetime is needed [173,174]. Thus, stable NPLs and device architectures are required to urgent be investigated. By overcoming these obstructions, more high-performance NPL-LEDs may be expected, which is beneficial for the next-generation display and lighting field.

Author Contributions: P.X., D.Y., D.L. and B.L. conceived the idea; P.X., J.H., D.Y., D.L., J.Y., D.L. and B.L. wrote the paper, P.X. and B.L. advised the paper. All authors reviewed the paper.

Funding: This research was funded by Scientific Research Starting Foundation of Foshan University (Grant No. Gg040926, 040928, 040973), the National Natural Science Foundation of China (Grant No. 61704027), the Foshan Science and Technology Innovation Special Funds (Grant No. 2017EZ100111), the National Natural Science Foundation of China (Grant No. 61704034), the Key Platforms and Research Projects of Department of Education of Guangdong Province (Grant No. 2016KTSCX034), the Guangdong Science and Technology Plan (Grant No. 2017B010123002).

Conflicts of Interest: The authors declare no conflicts of interest.

References

1. Tang, C.W.; VanSlyke, V.A. Organic Electroluminescent Diodes. *Appl. Phys. Lett.* **1987**, *51*, 913–915. [[CrossRef](#)]
2. Burroughes, J.H.; Bradley, D.D.C.; Brown, A.R.; Marks, R.N.; Mackay, K.; Friend, R.H.; Burns, P.L.; Homes, A.B. Light-Emitting Diodes Based on Conjugated Polymers. *Nature* **1990**, *347*, 539–541. [[CrossRef](#)]
3. Colvin, V.L.; Schlamp, M.C.; Alivisatos, A.P. Light-Emitting Diodes Made from Cadmium Selenide Nanocrystals and a Semiconducting Polymer. *Nature* **1994**, *370*, 354–357. [[CrossRef](#)]
4. Talapin, D.V.; Lee, J.-S.; Kovalenko, M.V.; Shevchenko, E.V. Prospects of Colloidal Nanocrystals for Electronic and Optoelectronic Applications. *Chem. Rev.* **2010**, *110*, 389–458. [[CrossRef](#)] [[PubMed](#)]
5. Stranks, S.D.; Snaith, H.J. Metal-Halide Perovskites for Photovoltaic and Light-Emitting Devices. *Nat. Nanotechnol.* **2015**, *10*, 391–402. [[CrossRef](#)] [[PubMed](#)]
6. Jing, L.; Kershaw, S.V.; Li, Y.; Huang, X.; Li, Y.; Rogach, A.L.; Gao, M. Aqueous Based Semiconductor Nanocrystals. *Chem. Rev.* **2016**, *116*, 10623–10730. [[CrossRef](#)] [[PubMed](#)]
7. Sutherland, B.R.; Sargent, E.H. Perovskite photonic sources. *Nat. Photonics* **2016**, *10*, 295–302. [[CrossRef](#)]

8. Sun, Q.J.; Wang, Y.A.; Li, L.S.; Wang, D.; Zhu, T.; Xu, J.; Yang, C.; Li, Y. Bright, Multicoloured Light-emitting Diodes Based on Quantum Dots. *Nat. Photonics* **2007**, *1*, 717–722. [[CrossRef](#)]
9. Yang, Y.X.; Zheng, Y.; Cao, W.R.; Titov, A.; Hyvonen, J.; Manders, J.R.; Xue, J.G.; Holloway, P.H.; Qian, L. High-Efficiency Light-Emitting Devices Based on Quantum Dots with Tailored Nanostructures. *Nat. Photonics* **2015**, *9*, 259–266. [[CrossRef](#)]
10. Ithurria, S.; Tessier, M.D.; Mahler, B.; Lobo, R.P.S.M.; Dubertret, B.; Efros, A.L. Colloidal Nanoplatelets with Two Dimensional Electronic Structure. *Nat. Mater.* **2011**, *10*, 936–941. [[CrossRef](#)] [[PubMed](#)]
11. Grim, J.Q.; Christodoulou, S.; Di Stasio, F.; Krahn, R.; Cingolani, R.; Manna, L.; Moreels, I. Continuous-Wave Biexciton Lasing at Room Temperature Using Solution-Processed Quantum Wells. *Nat. Nanotechnol.* **2014**, *9*, 891–895. [[CrossRef](#)] [[PubMed](#)]
12. Rowland, C.E.; Fedin, I.; Zhang, H.; Gray, S.K.; Govorov, A.O.; Talapin, D.V.; Schaller, R.D. Picosecond Energy Transfer and Multiexciton Transfer Outpaces Auger Recombination in Binary CdSe Nanoplatelet Solids. *Nat. Mater.* **2015**, *14*, 484–489. [[CrossRef](#)] [[PubMed](#)]
13. Riedinger, A.; Ott, F.D.; Mule, A.; Mazzotti, S.; Knusel, P.N.; Kress, S.J.P.; Prins, F.; Erwin, S.C.; Norris, D.J. An Intrinsic Growth Instability Inisotropic Materials Leads to Quasi-Two-Dimensional Nanoplatelets. *Nat. Mater.* **2017**, *16*, 743–748. [[PubMed](#)]
14. Mahler, B.; Nadal, B.; Bouet, C.; Patriarche, G.; Dubertret, B. Core/Shell Colloidal Semiconductor Nanoplatelets. *J. Am. Chem. Soc.* **2012**, *134*, 18591–18598. [[CrossRef](#)] [[PubMed](#)]
15. Prudnikau, A.; Chuvilin, A.; Artemyev, M. CdSe-CdS Nanoheteroplatelets with Efficient Photoexcitation of Central CdSe Region through Epitaxially Grown CdS Wings. *J. Am. Chem. Soc.* **2013**, *135*, 14476–14479. [[CrossRef](#)] [[PubMed](#)]
16. Tessier, M.D.; Spinicelli, P.; Dupont, D.; Patriarche, G.; Ithurria, S.; Dubertret, B. Efficient Exciton Concentrators Built from Colloidal Core/Crown CdSe/CdS Semiconductor Nanoplatelets. *Nano Lett.* **2014**, *14*, 207–213. [[CrossRef](#)] [[PubMed](#)]
17. Tessier, M.D.; Javaux, C.; Maksimovic, I.; Loriette, V.; Dubertret, B. Spectroscopy of Single CdSe Nanoplatelets. *ACS Nano* **2012**, *6*, 6751–6758. [[CrossRef](#)] [[PubMed](#)]
18. Wu, K.; Li, Q.; Jia, Y.; McBride, J.R.; Xie, Z.-X.; Lian, T. Efficient and Ultrafast Formation of Long-Lived Charge-Transfer Exciton State in Atomically Thin Cadmium Selenide/Cadmium Telluride Type-II Heteronanosheets. *ACS Nano* **2015**, *9*, 961–968. [[CrossRef](#)] [[PubMed](#)]
19. Kelestemur, Y.; Guzel Turk, B.; Erdem, O.; Olutas, M.; Gungor, K.; Demir, H.V. Platelet-in-Box Colloidal Quantum Wells: CdSe/CdS@CdS Core/Crown@Shell Heteronanoplatelets. *Adv. Funct. Mater.* **2016**, *26*, 3570–3579. [[CrossRef](#)]
20. Kunneman, L.T.; Schins, J.M.; Pedetti, S.; Heuclin, H.; Grozema, F.C.; Houtepen, A.J.; Dubertret, B.; Siebbeles, L.D.A. Nature and Decay Pathways of Photoexcited States in CdSe and CdSe/CdS Nanoplatelets. *Nano Lett.* **2014**, *14*, 7039–7045. [[CrossRef](#)] [[PubMed](#)]
21. She, C.; Fedin, I.; Dolzhenkov, D.S.; Dahlberg, P.D.; Engel, G.S.; Schaller, R.D.; Talapin, D.V. Red, Yellow, Green and Blue Amplified Spontaneous Emission and Lasing Using Colloidal CdSe Nanoplatelets. *ACS Nano* **2015**, *9*, 9475–9485. [[CrossRef](#)] [[PubMed](#)]
22. Rabouw, F.T.; Bok, J.C.; Spinicelli, P.; Mahler, B.; Nasilowski, M.; Pedetti, S.; Dubertret, B.; Vanmaekelbergh, D. Temporary Charge Carrier Separation Dominates the Photoluminescence Decay Dynamics of Colloidal CdSe Nanoplatelets. *Nano Lett.* **2016**, *16*, 2047–2053. [[CrossRef](#)] [[PubMed](#)]
23. Joo, J.; Son, J.S.; Kwon, S.G.; Yu, J.H.; Hyeon, T. Low-Temperature Solution-Phase Synthesis of Quantum Well Structured CdSe Nanoribbons. *J. Am. Chem. Soc.* **2006**, *128*, 5632–5633. [[CrossRef](#)] [[PubMed](#)]
24. Lhuillier, E.; Pedetti, S.; Ithurria, S.; Nadal, B.; Heuclin, H.; Dubertret, B. Two-Dimensional Colloidal Metal Chalcogenides Semiconductors: Synthesis, Spectroscopy, and Applications. *Acc. Chem. Res.* **2015**, *48*, 22–30. [[CrossRef](#)] [[PubMed](#)]
25. Bouet, C.; Tessier, M.D.; Ithurria, S.; Mahler, B.; Nadal, B.; Dubertret, B. Flat Colloidal Semiconductor Nanoplatelets. *Chem. Mater.* **2013**, *25*, 1262–1271. [[CrossRef](#)]
26. Dufour, M.; Steinmetz, V.; Izquierdo, E.; Pons, T.; Lequeux, N.; Lhuillier, E.; Legrand, L.; Chamarro, M.; Barisien, T.; Ithurria, J. Engineering Bicolor Emission in 2D Core/Crown CdSe/CdSe_{1-x}Tex Nanoplatelet Heterostructures Using Band-Offset Tuning. *J. Phys. Chem. C* **2017**, *121*, 24816–24823. [[CrossRef](#)]
27. Yang, J.; Son, S.J.; Yu, H.J.; Joo, J.; Hyeon, T. Advances in the Colloidal Synthesis of Two-Dimensional Semiconductor Nanoribbons. *Chem. Mater.* **2013**, *25*, 1190–1198. [[CrossRef](#)]

28. Tessier, M.D.; Mahler, B.; Nadal, B.; Heuclin, H.; Pedetti, S.; Dubertret, B. Spectroscopy of Colloidal Semiconductor Core/Shell Nanoplatelets with High Quantum Yield. *Nano Lett.* **2013**, *13*, 3321–3328. [[CrossRef](#)] [[PubMed](#)]
29. She, C.; Fedin, I.; Dolzhenkov, D.S.; Demortiere, A.; Schaller, R.D.; Pelton, M.; Talapin, D.V. Low-Threshold Stimulated Emission Using Colloidal Quantum Wells. *Nano Lett.* **2014**, *14*, 2772–2777. [[CrossRef](#)] [[PubMed](#)]
30. Olutas, M.; Guzelturk, B.; Kelestemur, Y.; Yeltik, A.; Delikanli, S.; Demir, H.V. Lateral Size-Dependent Spontaneous and Stimulated Emission Properties in Colloidal CdSe Nanoplatelets. *ACS Nano* **2015**, *9*, 5041–5050. [[CrossRef](#)] [[PubMed](#)]
31. Pedetti, S.; Ithurria, S.; Heuclin, H.; Patriarche, G.; Dubertret, B. Type-II CdSe/CdTe Core/Crown Semiconductor Nanoplatelets. *J. Am. Chem. Soc.* **2014**, *136*, 16430–16438. [[CrossRef](#)] [[PubMed](#)]
32. Li, Q.; Xu, Z.; McBride, J.R.; Lian, T. Colloidal CdSe/CdTe Core/Crown Type-II Nanoplatelet Heterostructures. *ACS Nano* **2017**, *11*, 2545–2553. [[CrossRef](#)] [[PubMed](#)]
33. Kelestemur, Y.; Guzelturk, B.; Erdem, O.; Olutas, M.; Erdem, T.; Usanmaz, C.F.; Gungor, K.; Demir, H.V. CdSe/CdSe_{1-x}Te_x Core/Crown Heteronoplatelets: Tuning the Excitonic Properties without Changing the Thickness. *J. Phys. Chem. C* **2017**, *121*, 4650–4658. [[CrossRef](#)]
34. Li, Q.; Zhou, B.; McBride, J.R.; Lian, T. Efficient Diffusive Transport of Hot and Cold Excitons in Colloidal Type II CdSe/CdTe Core/Crown Nanoplatelet Heterostructures. *ACS Energy Lett.* **2017**, *2*, 174–181. [[CrossRef](#)]
35. Chen, Z.; Nadal, B.; Mahler, B.; Aubin, H.; Dubertret, B. Quasi-2D Colloidal Semiconductor Nanoplatelets for Narrow Electroluminescence. *Adv. Funct. Mater.* **2014**, *24*, 295–302. [[CrossRef](#)]
36. Fan, F.; Kanjanaboos, P.; Saravanapavanantham, M.; Beauregard, E.; Ingram, G.; Yassitepe, E.; Adachi, M.M.; Voznyy, O.; Johnston, A.K.; Walters, G.; et al. Colloidal CdSe_{1-x}S_xNanoplatelets with Narrow and Continuously-Tunable Electroluminescence. *Nano Lett.* **2015**, *15*, 4611–4615. [[CrossRef](#)] [[PubMed](#)]
37. Liu, B.; Delikanli, S.; Gao, Y.; Gungor, K.; Demir, H.V. Nanocrystal light-emitting diodes based on type II nanoplatelets. *Nano Energy* **2018**, *47*, 115–122. [[CrossRef](#)]
38. Dai, X.L.; Zhang, Z.X.; Jin, Y.Z.; Niu, Y.; Cao, H.J.; Liang, X.Y.; Chen, L.W.; Wang, J.P.; Peng, X.G. Solution-Processed, High Performance Light-Emitting Diodes Based on Quantum Dots. *Nature* **2014**, *515*, 96–100. [[CrossRef](#)] [[PubMed](#)]
39. Yang, X.; Zhou, G.; Wong, W.-Y. Functionalization of Phosphorescent Emitters and Their Host Materials by Main-Group Elements for Phosphorescent Organic Light-Emitting Devices. *Chem. Soc. Rev.* **2015**, *44*, 8484–8575. [[CrossRef](#)] [[PubMed](#)]
40. Tyan, Y.S. Organic Light-Emitting-Diode Lighting Overview. *J. Photonics Energy* **2011**, *1*, 011009. [[CrossRef](#)]
41. Liu, B.; Gao, D.; Wang, J.; Wang, X.; Wang, L.; Zou, J.; Ning, H.; Peng, J. Progress of White Organic Light-Emitting Diodes. *Acta Phys. Chim. Sin.* **2015**, *31*, 1823–1852.
42. Yang, X.; Zhou, G.; Wong, W.-Y. Recent Design Tactics for High Performance White Polymer Light-Emitting Diodes. *J. Mater. Chem. C* **2014**, *2*, 1760–1778. [[CrossRef](#)]
43. Jou, J.-H.; Kumar, S.; Agrawal, A.; Li, T.-H.; Sahoo, S. Approaches for Fabricating High Efficiency Organic Light Emitting Diodes. *J. Mater. Chem. C* **2015**, *3*, 2974–3002. [[CrossRef](#)]
44. Sasabe, H.; Kido, J. Development of High Performance OLEDs for General Lighting. *J. Mater. Chem. C* **2013**, *1*, 1699–1707. [[CrossRef](#)]
45. Wang, Q.; Ma, D. Management of Charges and Excitons for High-performance White Organic Light-emitting Diodes. *Chem. Soc. Rev.* **2010**, *39*, 2387–2398. [[CrossRef](#)] [[PubMed](#)]
46. Liu, B.; Li, X.; Tao, H.; Zou, J.; Xu, M.; Wang, L.; Peng, J.; Cao, Y. Manipulation of Exciton Distribution for High-Performance Fluorescent/Phosphorescent Hybrid White Organic Light-Emitting Diodes. *J. Mater. Chem. C* **2017**, *5*, 7668–7683. [[CrossRef](#)]
47. Zhang, L.; Li, X.-L.; Luo, D.; Xiao, P.; Xiao, W.; Song, Y.; Ang, Q.; Liu, B. Strategies to Achieve High-Performance White Organic Light-Emitting Diodes. *Materials* **2017**, *10*, 1378. [[CrossRef](#)] [[PubMed](#)]
48. Xiao, P.; Dong, T.; Xie, J.; Luo, D.; Yuan, J.; Liu, B. Emergence of White Organic Light-Emitting Diodes Based on Thermally Activated Delayed Fluorescence. *Appl. Sci.* **2018**, *8*, 299. [[CrossRef](#)]
49. Liang, D.; Peng, Y.; Fu, Y.; Shearer, M.J.; Zhang, J.; Zhai, J.; Zhang, Y.; Hamers, R.J.; Andrew, T.L.; Jin, S. Color-pure violet-light-emitting diodes based on layered lead halide perovskite nanoplates. *ACS Nano* **2016**, *10*, 6897–6904. [[CrossRef](#)] [[PubMed](#)]

50. Qin, C.; Matsushima, T.; Sandanayaka, A.S.; Tsuchiya, Y.; Adachi, C. Centrifugal-Coated Quasi-Two-Dimensional Perovskite CsPb₂Br₅ Films for Efficient and Stable Light-Emitting Diodes. *J. Phys. Chem. Lett.* **2017**, *8*, 5415–5421. [[CrossRef](#)] [[PubMed](#)]
51. Ji, W.; Liu, S.; Zhang, H.; Wang, R.; Xie, W.; Zhang, H. Ultrasonic Spray Processed, Highly Efficient All-Inorganic Quantum-Dot Light-Emitting Diodes. *ACS Photonics* **2017**, *4*, 1271–1278. [[CrossRef](#)]
52. Ou, Q.D.; Zhou, L.; Li, Y.Q.; Chen, S.; Chen, J.D.; Li, C.; Wang, Q.K.; Lee, S.T.; Tang, J.X. Light-Emitting Diodes: Extremely Efficient White Organic Light-Emitting Diodes for General Lighting. *Adv. Funct. Mater.* **2014**, *24*, 7249–7256. [[CrossRef](#)]
53. Liu, B.; Lan, L.; Zou, J.; Peng, J. A novel organic light-emitting diode by utilizing double hole injection layer. *Acta Phys. Sin.* **2013**, *62*, 087302.
54. Liu, B.; Luo, D.; Gao, D.; Wang, X.; Xu, M.; Zou, J.; Ning, H.; Wang, L.; Peng, J.; Cao, Y. An ideal host-guest system to accomplish high-performance greenishyellow and hybrid white organic light-emitting diodes. *Org. Electron.* **2015**, *27*, 29–34. [[CrossRef](#)]
55. Wu, S.F.; Li, S.H.; Wang, Y.K.; Huang, C.C.; Sun, Q.; Liang, J.J.; Liao, L.S.; Fung, M.-K. White Organic LED with a Luminous Efficacy Exceeding 100 lm w⁻¹ without Light Out-Coupling Enhancement Techniques. *Adv. Funct. Mater.* **2017**, *27*, 1701314. [[CrossRef](#)]
56. Jou, J.-H.; Hsieh, C.-Y.; Tseng, J.-R.; Peng, S.-H.; Jou, Y.-C.; Hong, J.H.; Shen, S.-M.; Tang, M.-C.; Chen, P.-C.; Lin, C.-H. Candle Light-Style Organic Light-Emitting Diodes. *Adv. Funct. Mater.* **2013**, *23*, 2750–2757. [[CrossRef](#)]
57. Liu, B.; Wang, L.; Gao, D.Y.; Xu, M.; Zhu, X.H.; Zou, J.H.; Lan, L.F.; Ning, H.L.; Peng, J.B.; Cao, Y. Harnessing charge and exciton distribution towards extremely high performance: The critical role of guests in single-emitting-layer white OLEDs. *Mater. Horiz.* **2015**, *2*, 536–544. [[CrossRef](#)]
58. Liu, B.; Zou, J.H.; Zhou, Z.W.; Wang, L.; Xu, M.; Tao, H.; Gao, D.Y.; Lan, L.Y.; Ning, H.L.; Peng, J.B. Efficient single-emitting layer hybrid white organic light-emitting diodes with low efficiency roll-off, stable color and extremely high luminance. *J. Ind. Eng. Chem.* **2015**, *30*, 85–91. [[CrossRef](#)]
59. Liu, B.; Xu, M.; Wang, L.; Tao, H.; Su, Y.J.; Gao, D.Y.; Lan, L.F.; Zou, J.H.; Peng, J.B. Simplified hybrid white organic light-emitting diodes with efficiency/efficiency roll-off/color rendering index/color-stability trade-off. *Phys. Status Solidi RRL* **2014**, *8*, 719–723. [[CrossRef](#)]
60. Li, J.; Xu, L.; Wang, T.; Song, J.; Chen, J.; Xue, J.; Dong, Y.; Cai, B.; Shan, G.; Han, B.; et al. 50-Fold EQE Improvement up to 6.27% of Solution-Processed All-Inorganic Perovskite CsPbBr₃ QLEDs via Surface Ligand Density Control. *Adv. Mater.* **2017**, *29*, 1603885.
61. Liu, B.; Wang, L.; Gu, H.; Sun, H.; Demir, H.V. Highly Efficient Green Light-Emitting Diodes from All-Inorganic Perovskite Nanocrystals Enabled by a New Electron Transport Layer. *Adv. Opt. Mater.* **2018**. [[CrossRef](#)]
62. Wang, L.; Liu, B.; Zhao, X.; Demir, D.V.; Gu, H.; Sun, H. Solvent-Assisted Surface Engineering for High Performance All-Inorganic Perovskite Nanocrystals Light-Emitting Diodes. *ACS Appl. Mater. Interfaces* **2018**. [[CrossRef](#)] [[PubMed](#)]
63. Jiang, C.; Zhong, Z.; Liu, B.; He, Z.; Zou, J.; Wang, L.; Wang, J.; Peng, J.B.; Cao, Y. Coffee-Ring-Free Quantum Dot Thin Film Using Inkjet Printing from a Mixed-Solvent System on Modified ZnO Transport Layer for Light-Emitting Devices. *ACS Appl. Mater. Interfaces* **2016**, *8*, 26162–26168. [[CrossRef](#)] [[PubMed](#)]
64. Jiang, C.; Liu, H.; Liu, B.; Zhong, Z.; Zou, J.; Wang, J.; Wang, L.; Peng, J.; Cao, Y. Improved performance of inverted quantum dots light emitting devices by introducing double hole transport layers. *Org. Electron.* **2016**, *31*, 82–89. [[CrossRef](#)]
65. Rastogi, P.; Palazon, F.; Prato, M.; Stasio, F.D.; Krahne, R. Enhancing the Performance of CdSe/CdS Dot-in-Rod Light-Emitting Diodes via Surface Ligand Modification. *ACS Appl. Mater. Interfaces* **2018**, *10*, 5665–5672. [[CrossRef](#)] [[PubMed](#)]
66. Supran, G.J.; Shirasaki, Y.; Song, K.W.; Caruge, J.-M.; Kazlas, P.T.; Coe-Sullivan, S.; Andrew, T.L.; Bawendi, M.G.; Bulovic, V. QLEDs for displays and solid-state lighting. *MRS Bull.* **2013**, *38*, 703–711. [[CrossRef](#)]
67. Mashford, B.S.; Stevenson, M.; Popovic, Z.; Hamilton, C.; Zhou, Z.; Breen, C.; Steckel, J.; Bulovic, V.; Bawendi, M.; Coe-Sullivan, S.; et al. High-efficiency quantum-dot light-emitting devices with enhanced charge injection. *Nat. Photonics* **2013**, *7*, 407–412. [[CrossRef](#)]

68. Coe, S.; Woo, W.-K.; Bawendi, M.G.; Bulovic, V. Electro-luminescence from Single Monolayers of Nanocrystals in Molecular Organic Devices. *Nature* **2002**, *420*, 800–803. [[CrossRef](#)] [[PubMed](#)]
69. Shirasaki, Y.; Supran, G.J.; Bawendi, M.G.; Bulović, V. Emergence of colloidal quantum-dot light-emitting technologies. *Nat. Photonics* **2013**, *7*, 13–23. [[CrossRef](#)]
70. Higuchi, T.; Nakanotani, H.; Adachi, C. High-Efficiency White Organic Light-Emitting Diodes Based on a Blue Thermally Activated Delayed Fluorescent Emitter Combined with Green and Red Fluorescent Emitters. *Adv. Mater.* **2015**, *27*, 2019–2023. [[CrossRef](#)] [[PubMed](#)]
71. Liu, B.; Wang, L.; Gao, D.Y.; Zou, J.H.; Ning, H.L.; Peng, J.B.; Cao, Y. Extremely high-efficiency and ultrasimplified hybrid white organic light-emitting diodes exploiting double multifunctional blue emitting layers. *Light Sci. Appl.* **2016**, *5*, e16137. [[CrossRef](#)]
72. Liu, B.; Nie, H.; Zhou, X.B.; Hu, S.B.; Luo, D.X.; Gao, D.Y.; Zou, J.H.; Xu, M.; Wang, L.; Zhao, Z.J.; et al. Manipulation of Charge and Exciton Distribution Based on Blue Aggregation-Induced Emission Fluorophors: A Novel Concept to Achieve High-Performance Hybrid White Organic Light-Emitting Diodes. *Adv. Funct. Mater.* **2016**, *26*, 776–783. [[CrossRef](#)]
73. Reineke, S.; Lindner, F.; Schwartz, G.; Seidler, N.; Walzer, K.; Lüssem, B.; Leo, K. White organic light-emitting diodes with fluorescent tube efficiency. *Nature* **2009**, *459*, 234–238. [[CrossRef](#)] [[PubMed](#)]
74. Kim, D.Y.; Park, J.H.; Lee, J.W.; Hwang, S.; Oh, S.J.; Kim, J.; Sone, C.; Schubert, E.F.; Kim, J.K. Overcoming the fundamental light-extraction efficiency limitations of deep ultraviolet light-emitting diodes by utilizing transverse-magnetic-dominant emission. *Light Sci. Appl.* **2015**, *4*, e263. [[CrossRef](#)]
75. Preinfalk, J.B.; Eiselt, T.; Wehlius, T.; Rohnacher, V.; Hanemann, T.; Gomard, G.; Lemmer, U. Large-Area Screen-Printed Internal Extraction Layers for Organic Light-Emitting Diodes. *ACS Photonics* **2017**, *4*, 928–933. [[CrossRef](#)]
76. Koh, T.-W.; Spechler, J.A.; Lee, K.M.; Arnold, C.B.; Rand, B.P. Enhanced Outcoupling in Organic Light-Emitting Diodes via a High-Index Contrast Scattering Layer. *ACS Photonics* **2015**, *2*, 1366–1372. [[CrossRef](#)]
77. Liu, B.; Wang, L.; Xu, M.; Tao, H.; Gao, D.; Zou, J.; Lan, L.; Ning, H.; Peng, J.; Cao, Y. Extremely Stable-color Flexible White Organic Light-emitting Diodes with Efficiency Exceeding 100 lm W⁻¹. *J. Mater. Chem. C* **2014**, *2*, 9836–9841. [[CrossRef](#)]
78. Hong, T.; Gao, D.; Liu, B.; Wang, L.; Zou, J.; Xu, M.; Peng, J. Enhancement of tandem organic light-emitting diode performance by inserting an ultra-thin Ag layer in charge generation layer. *Acta Phys. Sin.* **2017**, *1*, 017302.
79. Liu, B.; Wang, L.; Xu, M.; Tao, H.; Xia, X.; Zou, J.; Su, Y.; Gao, D.; Lan, L.; Peng, J. Simultaneous Achievement of Low Efficiency Roll-Off and Stable Color in Highly Efficient Single-Emitting-Layer Phosphorescent White Organic Light-Emitting Diodes. *J. Mater. Chem. C* **2014**, *2*, 5870–5877. [[CrossRef](#)]
80. Liu, B.; Wang, L.; Zou, J.H.; Tao, H.; Su, Y.J.; Gao, D.Y.; Xu, M.; Lan, L.F.; Peng, J.B. Investigation on spacers and structures: A simple but effective approach toward high-performance hybrid white organic light emitting diodes. *Synth. Met.* **2013**, *184*, 5–9. [[CrossRef](#)]
81. Luo, D.; Yang, Y.F.; Xiao, Y.; Zhao, Y.; Yang, Y.B.; Liu, B.Q. Regulating Charge and Exciton Distribution in High-Performance Hybrid White Organic Light-Emitting Diodes with n-Type Interlayer Switch. *Nano-Micro Lett.* **2017**, *9*, 37. [[CrossRef](#)]
82. Fröbel, M.; Schwab, T.; Kliem, M.; Hofmann, S.; Leo, K.; Gather, M.C. Get It White: Color-Tunable Ac/Dc OLEDs. *Light Sci. Appl.* **2015**, *4*, e247. [[CrossRef](#)]
83. Liu, B.; Xu, M.; Wang, L.; Zou, J.H.; Tao, H.; Su, Y.J.; Gao, D.Y.; Ning, H.L.; Lan, L.F.; Peng, J.B. Regulating charges and excitons in simplified hybrid white organic light-emitting diodes: The key role of concentration in single dopant host-guest systems. *Org. Electron.* **2014**, *15*, 2616–2623. [[CrossRef](#)]
84. Liu, B.; Xu, M.; Wang, L.; Su, Y.J.; Gao, D.Y.; Tao, H.; Lan, L.F.; Zou, J.H.; Peng, J.B. High-Performance Hybrid White Organic Light-Emitting Diodes Comprising Ultrathin Blue and Orange Emissive Layers. *Appl. Phys. Express* **2013**, *6*, 122101. [[CrossRef](#)]
85. Liu, B.; Xu, M.; Wang, L.; Tao, H.; Su, Y.; Gao, D.; Lan, L.; Zou, J.; Peng, J. Very-High Color Rendering Index Hybrid White Organic Light-Emitting Diodes with Double Emitting Nanolayers. *Nano-Micro Lett.* **2014**, *6*, 335–339. [[CrossRef](#)]

86. Su, S.-J.; Gonmori, E.; Sasabe, H.; Kido, J. Highly efficient organic blue- and white-light-emitting devices having a carrier- and exciton-confining structure for reduced efficiency roll-off. *Adv. Mater.* **2008**, *20*, 4189–4194. [[CrossRef](#)]
87. Schwartz, G.; Ke, T.-H.; Wu, C.-C.; Walzer, K.; Leo, K. Balanced ambipolar charge carrier mobility in mixed layers for application in hybrid white organic light-emitting diodes. *Appl. Phys. Lett.* **2008**, *93*, 073304. [[CrossRef](#)]
88. Schwartz, G.; Reineke, S.; Walzer, K.; Leo, K. Reduced efficiency roll-off in high-efficiency hybrid white organic light-emitting diodes. *Appl. Phys. Lett.* **2008**, *92*, 053311. [[CrossRef](#)]
89. Peng, Q.M.; Chen, P.; Sun, J.X.; Li, F. Magnetic field effects on electroluminescence emanated simultaneously from blue fluorescent and red phosphorescent emissive layers of an organic light-emitting diode. *Org. Electron.* **2012**, *13*, 3040–3044. [[CrossRef](#)]
90. Zhao, F.C.; Zhang, Z.Q.; Liu, Y.P.; Dai, Y.F.; Chen, J.S.; Ma, D.G. A hybrid white organic light-emitting diode with stable color and reduced efficiency roll-off by using a bipolar charge carrier switch. *Org. Electron.* **2012**, *13*, 1049–1055. [[CrossRef](#)]
91. Chen, Y.; Zhao, F.; Zhao, Y.; Chen, J.; Ma, D. Ultra-simple hybrid white organic light-emitting diodes with high efficiency and CRI trade-off: Fabrication and emission-mechanism analysis. *Org. Electron.* **2012**, *13*, 2807–2815. [[CrossRef](#)]
92. Vitukhnovsky, A.G.; Lebedev, V.S.; Selyukov, A.S.; Vashchenko, A.A.; Vasiliev, R.B.; Sokolikova, M.S. Electroluminescence from colloidal semiconductor CdSe nanoplatelets in hybrid organic–inorganic light emitting diode. *Chem. Phys. Lett.* **2015**, *619*, 185–188. [[CrossRef](#)]
93. Ithurria, S.; Dubertret, B. Quasi 2D Colloidal CdSe Platelets with Thicknesses Controlled at the Atomic Level. *J. Am. Chem. Soc.* **2008**, *130*, 16504–16505. [[CrossRef](#)] [[PubMed](#)]
94. Li, Z.; Qin, H.; Guzun, D.; Benamara, M.; Salamo, G.; Peng, X. Uniform thickness and colloidal-stable CdS quantum disks with tunable thickness: Synthesis and properties. *Nano Res.* **2012**, *5*, 337–351. [[CrossRef](#)]
95. Gao, Y.; Li, M.; Delikanli, S.; Zheng, H.; Liu, B.; Dang, C.; Sum, T.C.; Demir, H.V. Low-threshold lasing from colloidal CdSe/CdSeTe core/alloyed-crown type-II heteronoplatelets. *Nanoscale* **2018**, *10*, 9466–9475. [[CrossRef](#)] [[PubMed](#)]
96. Kim, S.; Fisher, B.; Eisler, H.-J.; Bawendi, M. Type-II quantum dots: CdTe/CdSe (core/shell) and CdSe/ZnTe (core/shell) heterostructures. *J. Am. Chem. Soc.* **2003**, *125*, 11466–11467. [[CrossRef](#)] [[PubMed](#)]
97. Liu, B.; Xu, Z.P.; Zou, J.H.; Tao, H.; Xu, M.; Gao, D.Y.; Lan, L.F.; Wang, L.; Ning, H.L.; Peng, J.B. High-performance hybrid white organic light-emitting diodes employing p-type interlayers. *J. Ind. Eng. Chem.* **2015**, *27*, 240–244. [[CrossRef](#)]
98. Liu, B.; Xu, M.; Wang, L.; Yan, X.; Tao, H.; Su, Y.; Gao, D.; Lan, L.; Zou, J.; Peng, J. Investigation and Optimization of Each Organic Layer: A Simple But Effective Approach Towards Achieving High-Efficiency Hybrid White Organic Light-Emitting Diodes. *Org. Electron.* **2014**, *15*, 926. [[CrossRef](#)]
99. Lee, M.M.; Teuscher, J.; Miyasaka, T.; Murakami, T.N.; Snaith, H.J. Efficient hybrid solar cells based on meso-superstructured organometal halide perovskites. *Science* **2012**, *338*, 643–647. [[CrossRef](#)] [[PubMed](#)]
100. Luo, J.; Im, J.H.; Mayer, M.T.; Schreier, M.; Nazeeruddin, M.K.; Park, N.G.; Tilley, S.D.; Fan, H.J.; Grätzel, M. Water photolysis at 12.3% efficiency via perovskite photovoltaics and Earth-abundant catalysts. *Science* **2014**, *345*, 1593–1596. [[PubMed](#)]
101. Jeon, N.J.; Noh, J.H.; Yang, W.S.; Kim, Y.C.; Ryu, S.; Seo, J.; Seok, S.I. Compositional engineering of perovskite materials for high-performance solar cells. *Nature* **2015**, *517*, 476–480. [[CrossRef](#)] [[PubMed](#)]
102. Zhu, H.; Fu, Y.; Meng, F.; Wu, X.; Gong, Z.; Ding, Q.; Gustafsson, M.V.; Trinh, M.T.; Jin, S.; Zhu, X.Y. Lead halide perovskite nanowire lasers with low lasing thresholds and high quality factors. *Nat. Mater.* **2015**, *14*, 636–642. [[CrossRef](#)] [[PubMed](#)]
103. Kojima, A.; Teshima, K.; Shirai, Y.; Miyasaka, T. Organometal halide perovskites as visible-light sensitizers for photovoltaic cells. *J. Am. Chem. Soc.* **2009**, *131*, 6050–6051. [[CrossRef](#)] [[PubMed](#)]
104. Ji, H.; Shi, Z.; Sun, X.; Li, Y.; Li, S.; Lei, L.; Wu, D.; Xu, T.; Li, X.; Du, G. Vapor-Assisted Solution Approach for High-Quality Perovskite CH₃NH₃PbBr₃ Thin Films for High-Performance Green Light-Emitting Diode Applications. *ACS Appl. Mater. Int.* **2017**, *9*, 42893–42904. [[CrossRef](#)] [[PubMed](#)]
105. Gao, P.; Grätzel, M.; Nazeeruddin, M.K. Organohalide lead perovskites for photovoltaic applications. *Energy Environ. Sci.* **2014**, *7*, 2448–2463. [[CrossRef](#)]

106. Shi, Z.; Li, Y.; Li, S.; Li, X.; Wu, D.; Xu, T.; Tian, Y.; Chen, Y.; Zhang, Y.; Zhang, B.; et al. Localized Surface Plasmon Enhanced All-Inorganic Perovskite Quantum Dot Light-Emitting Diodes Based on Coaxial Core/Shell Heterojunction Architecture. *Adv. Funct. Mater.* **2018**, *28*, 1707031. [[CrossRef](#)]
107. Tan, Z.K.; Moghaddam, R.S.; Lai, M.L.; Docampo, P.; Higler, R.; Deschler, F.; Price, M.; Sadhanala, A.; Pazos, L.M.; Credgington, D.; et al. Bright light-emitting diodes based on organometal halide perovskite. *Nat. Nanotechnol.* **2014**, *9*, 687–692. [[CrossRef](#)] [[PubMed](#)]
108. Cho, H.; Jeong, S.-H.; Park, M.-H.; Kim, Y.-H.; Wolf, C.; Lee, C.-L.; Heo, J.H.; Sadhanala, A.; Myoung, N.; Yoo, S.; et al. Overcoming the electroluminescence efficiency limitations of perovskite light-emitting diodes. *Science* **2015**, *350*, 1222–1225. [[CrossRef](#)] [[PubMed](#)]
109. Kim, Y.-H.; Cho, H.; Heo, J.H.; Kim, T.-S.; Myoung, N.; Lee, C.-L.; Im, S.H.; Lee, T.-W. Multicolored Organic/Inorganic Hybrid Perovskite Light-Emitting Diodes. *Adv. Mater.* **2015**, *27*, 1248–1254. [[CrossRef](#)] [[PubMed](#)]
110. Kim, Y.-H.; Cho, H.; Lee, T.-W. Metal halide perovskite light emitters. *Proc. Natl. Acad. Sci. USA* **2016**, *113*, 11694–11702. [[CrossRef](#)] [[PubMed](#)]
111. Hoye, R.L.Z.; Chua, M.R.; Musselman, K.P.; Li, G.; Lai, M.-L.; Tan, Z.-K.; Greenham, N.C.; MacManus-Driscoll, J.L.; Friend, R.H.; Credgington, D. Enhanced Performance in Fluorene-Free Organometal Halide Perovskite Light-Emitting Diodes using Tunable, Low Electron Affinity Oxide Electron Injectors. *Adv. Mater.* **2015**, *27*, 1414–1419. [[CrossRef](#)] [[PubMed](#)]
112. Wang, J.; Wang, N.; Jin, Y.; Si, J.; Tan, Z.-K.; Du, H.; Cheng, L.; Dai, X.; Bai, S.; He, H.; et al. Interfacial Control Toward Efficient and Low-Voltage Perovskite Light-Emitting Diodes. *Adv. Mater.* **2015**, *27*, 2311–2316. [[CrossRef](#)] [[PubMed](#)]
113. Yu, J.C.; Kim, D.B.; Baek, G.; Lee, B.R.; Jung, E.D.; Lee, S.; Chu, J.H.; Lee, D.-K.; Choi, K.J.; Cho, S.; et al. High-Performance Planar Perovskite Optoelectronic Devices: A Morphological and Interfacial Control by Polar Solvent Treatment. *Adv. Mater.* **2015**, *27*, 3492–3500. [[CrossRef](#)] [[PubMed](#)]
114. Wang, N.; Cheng, L.; Ge, R.; Zhang, S.; Miao, Y.; Zou, W.; Yi, C.; Sun, Y.; Cao, Y.; Yang, R.; et al. Perovskite Light-Emitting Diodes based on Solution-Processed, Self-Organised Multiple Quantum Wells. *Nat. Nanotechnol.* **2016**, *10*, 699–704.
115. Manser, J.S.; Christians, J.A.; Kamat, P.V. Intriguing Optoelectronic Properties of Metal Halide Perovskites. *Chem. Rev.* **2016**, *116*, 12956–13008. [[CrossRef](#)] [[PubMed](#)]
116. Quan, L.N.; Zhao, Y.; García de Arquer, F.P.; Sabatini, R.; Walters, G.; Voznyy, O.; Comin, R.; Li, Y.; Fan, J.Z.; Tan, H.; et al. Tailoring the Energy Landscape in Quasi-2D Halide Perovskites Enables Efficient Green-Light Emission. *Nano Lett.* **2017**, *17*, 3701–3709. [[CrossRef](#)] [[PubMed](#)]
117. Xiao, Z.; Kerner, R.A.; Zhao, L.; Tran, N.L.; Lee, K.M.; Koh, T.-W.; Scholes, G.D.; Rand, B.P. Efficient Perovskite Light-Emitting Diodes Featuring Nanometre-Sized Crystallites. *Nat. Photonics* **2017**, *11*, 108–115. [[CrossRef](#)]
118. Byun, J.; Cho, H.; Wolf, C.; Jang, M.; Sadhanala, A.; Friend, R.H.; Yang, H.; Lee, T.-W. Efficient Visible Quasi-2D Perovskite Light Emitting Diodes. *Adv. Mater.* **2016**, *28*, 7515–7520. [[CrossRef](#)] [[PubMed](#)]
119. Kitazawa, N.; Watanabe, Y. Optical Properties of Natural Quantum-Well Compounds (C₆H₅-C_nH_{2n}-NH₃)₂PbBr₄ (n = 1–4). *J. Phys. Chem. Solids* **2010**, *71*, 797–802. [[CrossRef](#)]
120. Dou, L.; Wong, A.B.; Yu, Y.; Lai, M.; Kornienko, N.; Eaton, S.W.; Fu, A.; Bischak, C.G.; Ma, J.; Ding, T.; et al. Atomically Thin Two-Dimensional Organic-Inorganic Hybrid Perovskites. *Science* **2015**, *349*, 1518–1521. [[CrossRef](#)] [[PubMed](#)]
121. Cheng, Z.; Lin, J. Layered Organic-Inorganic Hybrid Perovskites: Structure, Optical Properties, Film Preparation, Patterning and Templating Engineering. *CrystEngComm* **2010**, *12*, 2646–2662. [[CrossRef](#)]
122. Mitzi, D.B. Templating and Structural Engineering in Organic-Inorganic Perovskites. *J. Chem. Soc. Dalton Trans.* **2001**, *1*, 1–12. [[CrossRef](#)]
123. Saparov, B.; Mitzi, D.B. Organic-Inorganic Perovskites: Structural Versatility for Functional Materials Design. *Chem. Rev.* **2016**, *116*, 4558–4596. [[CrossRef](#)] [[PubMed](#)]
124. Liu, B.; Xu, M.; Tao, H.; Ying, L.; Zou, J.; Wu, H.; Peng, J. Highly Efficient Red Phosphorescent Organic Light-Emitting Diodes Based on Solution Processed Emissive Layer. *J. Lumin.* **2013**, *142*, 35–39. [[CrossRef](#)]
125. Luo, D.; Li, X.-L.; Zhao, Y.; Gao, Y.; Liu, B. High-Performance Blue Molecular Emitter-Free and Doping-Free Hybrid White Organic Light-Emitting Diodes: An Alternative Concept to Manipulate Charges and Excitons Based on Exciplex and Electroplex Emission. *ACS Photonics* **2017**, *4*, 1566–1575. [[CrossRef](#)]

126. Luo, D.; Yang, Y.B.; Huang, L.; Liu, B.Q.; Zhao, Y. High-performance hybrid white organic light-emitting diodes exploiting blue thermally activated delayed fluorescent dyes. *Dyes Pigments* **2017**, *147*, 83–89. [[CrossRef](#)]
127. Ling, Y.; Yuan, Z.; Tian, Y.; Wang, X.; Wang, J.C.; Xin, Y.; Hanson, K.; Ma, B.; Gao, H. Bright Light-Emitting Diodes Based on Organometal Halide Perovskite Nanoplatelets. *Adv. Mater.* **2016**, *28*, 305–311. [[CrossRef](#)] [[PubMed](#)]
128. Si, J.; Liu, Y.; He, Z.; Du, H.; Du, K.; Chen, D.; Li, J.; Xu, M.; Tian, H.; He, H.; et al. Efficient and High-Color-Purity Light-Emitting Diodes Based on In Situ Grown Films of CsPbX₃ (X = Br, I) Nanoplates with Controlled Thicknesses. *ACS Nano* **2017**, *11*, 11100–11107. [[CrossRef](#)] [[PubMed](#)]
129. Protesescu, L.; Yakunin, S.; Bodnarchuk, M.I.; Krieg, F.; Caputo, R.; Hendon, C.H.; Yang, R.X.; Walsh, A.; Kovalenko, M.V. Nanocrystals of Cesium Lead Halide Perovskites (CsPbX₃, X = Cl, Br, and I): Novel Optoelectronic Materials Showing Bright Emission with Wide Color Gamut. *Nano Lett.* **2015**, *15*, 3692–3696. [[CrossRef](#)] [[PubMed](#)]
130. Yettapu, G.R.; Talukdar, D.; Sarkar, S.; Swarnkar, A.; Nag, A.; Ghosh, P.; Mandal, P. Terahertz Conductivity within Colloidal CsPbBr₃ Perovskite Nanocrystals: Remarkably High Carrier Mobilities and Large Diffusion Lengths. *Nano Lett.* **2016**, *16*, 4838–4848. [[CrossRef](#)] [[PubMed](#)]
131. Pan, A.; He, B.; Fan, X.; Liu, Z.; Urban, J.J.; Alivisatos, A.P.; He, L.; Liu, Y. Insight into the Ligand-Mediated Synthesis of Colloidal CsPbBr₃ Perovskite Nanocrystals: The Role of Organic Acid, Base, and Cesium Precursors. *ACS Nano* **2016**, *10*, 7943–7954. [[CrossRef](#)] [[PubMed](#)]
132. Pan, J.; Quan, L.N.; Zhao, Y.; Peng, W.; Murali, B.; Sarmah, S.P.; Yuan, M.; Sinatra, L.; Alyami, N.M.; Liu, J.; et al. Highly Efficient Perovskite-Quantum-Dot Light-Emitting Diodes by Surface Engineering. *Adv. Mater.* **2016**, *28*, 8718–8725. [[CrossRef](#)] [[PubMed](#)]
133. Swarnkar, A.; Marshall, A.R.; Sanehira, E.M.; Chernomordik, B.D.; Moore, D.T.; Christians, J.A.; Chakrabarti, T.; Luther, J.M. Quantum dot-induced phase stabilization of α -CsPbI₃ perovskite for high-efficiency photovoltaics. *Science* **2016**, *354*, 92–95. [[CrossRef](#)] [[PubMed](#)]
134. Shi, Z.; Li, Y.; Zhang, Y.; Chen, Y.; Li, X.; Wu, D.; Xu, T.; Shan, C.; Du, G. High-efficiency and air-stable perovskite quantum dots light-emitting diodes with an all-inorganic heterostructure. *Nano Lett.* **2016**, *17*, 313–321. [[CrossRef](#)] [[PubMed](#)]
135. Cho, H.; Wolf, C.; Kim, J.S.; Yun, H.J.; Bae, S.S.; Kim, H.; Heo, J.-M.; Ahn, S.; Lee, T.-W. High-Efficiency Solution-Processed Inorganic Metal Halide Perovskite Light-Emitting Diodes. *Adv. Mater.* **2017**, *29*, 1700579. [[CrossRef](#)] [[PubMed](#)]
136. Zhang, X.; Wang, W.; Xu, B.; Liu, S.; Dai, H.; Bian, D.; Chen, S.; Wang, K.; Sun, X.W. Thin film perovskite light-emitting diode based on CsPbBr₃ powders and interfacial engineering. *Nano Energy* **2017**, *37*, 40–45. [[CrossRef](#)]
137. Song, J.; Li, J.; Li, X.; Xu, L.; Dong, Y.; Zeng, H. Quantum dot light-emitting diodes based on inorganic perovskite cesium lead halides (CsPbX₃). *Adv. Mater.* **2015**, *27*, 7162–7167. [[CrossRef](#)] [[PubMed](#)]
138. Ling, Y.; Tian, Y.; Wang, X.; Wang, J.C.; Knox, J.M.; Perez-Orive, F.; Du, Y.; Tan, L.; Hanson, K.; Ma, B.; et al. Enhanced Optical and Electrical Properties of Polymer-Assisted All-Inorganic Perovskites for Light-Emitting Diodes. *Adv. Mater.* **2016**, *28*, 8983–8989. [[CrossRef](#)] [[PubMed](#)]
139. Wang, H.-C.; Wang, W.; Tang, A.-C.; Tsai, H.-Y.; Bao, Z.; Ihara, T.; Yarita, N.; Tahara, H.; Kanemitsu, T.; Chen, S.; et al. High-Performance CsPb_{1-x}Sn_xBr₃ Perovskite Quantum Dots for Light-Emitting Diodes. *Angew. Chem. Int. Ed.* **2017**, *129*, 13838–13842. [[CrossRef](#)]
140. Zhang, X.; Xu, B.; Zhang, J.; Gao, Y.; Zheng, Y.; Wang, K.; Sun, X.W. All-Inorganic Perovskite Nanocrystals for High-Efficiency Light Emitting Diodes: Dual-Phase CsPbBr₃-CsPb₂Br₅ Composites. *Adv. Funct. Mater.* **2016**, *26*, 4595–4600. [[CrossRef](#)]
141. Bekenstein, Y.; Koscher, B.A.; Eaton, S.W.; Yang, P.; Alivisatos, A.P. Highly luminescent colloidal nanoplates of perovskite cesium lead halide and their oriented assemblies. *J. Am. Chem. Soc.* **2015**, *137*, 16008–16011. [[CrossRef](#)] [[PubMed](#)]
142. Chen, S.; Shi, G. Two-dimensional materials for halide perovskite-based optoelectronic devices. *Adv. Mater.* **2017**, *29*, 1605448. [[CrossRef](#)] [[PubMed](#)]
143. Kormilina, T.K.; Chervkov, S.A.; Fedorov, A.V.; Baranov, A.V. Cadmium Chalcogenide Nano-Heteroplatelets: Creating Advanced Nanostructured Materials by Shell Growth, Substitution, and Attachment. *Small* **2017**, *13*, 1702300. [[CrossRef](#)] [[PubMed](#)]

144. Akkerman, Q.A.; Motti, S.G.; Srimath Kandada, A.R.; Mosconi, E.; D’Innocenzo, V.; Bertoni, G.; Marras, S.; Kamino, B.A.; Miranda, L.; De Angelis, F.; et al. Solution synthesis approach to colloidal cesium lead halide perovskite nanoplatelets with monolayer-level thickness control. *J. Am. Chem. Soc.* **2016**, *138*, 1010–1016. [[CrossRef](#)] [[PubMed](#)]
145. Song, J.; Xu, L.; Li, J.; Xue, J.; Dong, Y.; Li, X.; Zeng, H. Monolayer and few-layer allinorganic perovskites as a new family of two-dimensional semiconductors for printable optoelectronic devices. *Adv. Mater.* **2016**, *28*, 4861–4869. [[CrossRef](#)] [[PubMed](#)]
146. Shi, Z.; Li, S.; Li, Y.; Ji, H.; Li, X.; Wu, D.; Xu, T.; Chen, Y.; Tian, Y.; Zhang, Y.; et al. Strategy of solution-processed all-inorganic heterostructure for humidity/temperature-stable perovskite quantum dot light-emitting diodes. *ACS Nano* **2018**, *12*, 1462–1472. [[CrossRef](#)] [[PubMed](#)]
147. Schmidt, L.C.; Pertegas, A.; Gonzalez-Carrero, S.; Malinkiewicz, O.; Agouram, S.; Manguel Espallargas, G.; Bolink, H.J.; Galian, R.E.; Pérez-Prieto, J. Nontemplate Synthesis of CH₃NH₃PbBr₃ Perovskite Nanoparticles. *J. Am. Chem. Soc.* **2014**, *136*, 850–853. [[CrossRef](#)] [[PubMed](#)]
148. Wang, K.; Wu, L.; Li, L.; Yao, H.; Qian, H.; Yu, S. Large-Scale Synthesis of Highly Luminescent Perovskite-Related CsPb₂Br₅ Nanoplatelets and Their Fast Anion Exchange. *Angew. Chem., Int. Ed.* **2016**, *55*, 8328–8332. [[CrossRef](#)] [[PubMed](#)]
149. Tang, X.; Hu, Z.; Yuan, W.; Hu, W.; Shao, H.; Han, D.; Zheng, J.; Hao, J.; Zang, Z.; Du, J.; et al. Perovskite CsPb₂Br₅ Microplate Laser with Enhanced Stability and Tunable Properties. *Adv. Opt. Mater.* **2017**, *5*, 1600788. [[CrossRef](#)]
150. Ruan, L.; Shen, W.; Wang, A.; Xiang, A.; Deng, Z. Alkyl-Thiol Ligand-Induced Shape- and Crystalline Phase-Controlled Synthesis of Stable Perovskite-Related CsPb₂Br₅ Nanocrystals at Room Temperature. *J. Phys. Chem. Lett.* **2017**, *8*, 3853–3860. [[CrossRef](#)] [[PubMed](#)]
151. Nedelcu, G.; Protesescu, L.; Yakunin, S.; Bodnarchuk, M.I.; Grotevent, M.J.; Kovalenko, M.V. Fast anion-exchange in highly luminescent nanocrystals of cesium lead halide perovskites (CsPbX₃, X = Cl, Br, I). *Nano Lett.* **2015**, *15*, 5635–5640. [[CrossRef](#)] [[PubMed](#)]
152. Huang, H.; Liu, M.; Li, J.; Luo, L.; Zhao, J.; Luo, Z.; Wang, X.; Ye, Z.; He, H.; Zeng, J. Atomically thin cesium lead bromide perovskite quantum wires with high luminescence. *Nanoscale* **2017**, *9*, 104–108. [[CrossRef](#)] [[PubMed](#)]
153. Kumar, S.; Jagielski, J.; Yakunin, S.; Rice, P.; Chiu, Y.C.; Wang, M.; Nedelcu, G.; Kim, Y.; Lin, S.; Santos, E.J.; et al. Efficient blue electroluminescence quantum-confined two-dimensional perovskites. *ACS Nano* **2016**, *10*, 9720–9729. [[CrossRef](#)] [[PubMed](#)]
154. Alivisatos, A.P. Semiconductor clusters, nanocrystals, and quantum dots. *Science* **1996**, *271*, 933–937. [[CrossRef](#)]
155. Yang, D.; Zou, Y.; Li, P.; Liu, Q.; Wu, L.; Hu, H.; Xu, Y.; Sun, B.; Zhang, Q.; Lee, S.T. Large-scale synthesis of ultrathin cesium lead bromide perovskite nanoplates with precisely tunable dimensions and their application in blue light-emitting diodes. *Nano Energy* **2018**, *47*, 235–242. [[CrossRef](#)]
156. Yoshihiro, O. Color rendering and luminous efficacy of white LED spectra. *Proc. SPIE* **2004**, 5530. [[CrossRef](#)]
157. Liu, B.; Nie, H.; Lin, G.; Hu, S.; Gao, D.; Zou, J.; Xu, M.; Wang, L.; Zhao, Z.; Ning, H.; et al. High-Performance Doping-Free Hybrid White OLEDs Based on Blue Aggregation-Induced Emission Luminogens. *ACS Appl. Mater. Interfaces* **2017**, *9*, 34162–34171. [[CrossRef](#)] [[PubMed](#)]
158. Liu, B.; Tao, H.; Wang, L.; Gao, D.Y.; Liu, W.C.; Zou, J.H.; Xu, M.; Ning, H.L.; Peng, J.B.; Cao, Y. High-performance doping-free hybrid white organic light-emitting diodes: The exploitation of ultrathin emitting nanolayers (<1 nm). *Nano Energy* **2016**, *26*, 26–36. [[CrossRef](#)]
159. Liu, B.; Luo, D.X.; Zou, J.H.; Gao, D.Y.; Ning, H.L.; Wang, L.; Peng, J.B.; Cao, Y. A host-guest system comprising high guest concentration to achieve simplified and high-performance hybrid white organic light-emitting diodes. *J. Mater. Chem. C* **2015**, *3*, 6359–6366. [[CrossRef](#)]
160. Liu, B.; Tao, H.; Su, Y.J.; Gao, D.Y.; Lan, L.F.; Zou, J.H.; Peng, J.B. Color-stable, reduced efficiency roll-off hybrid white organic light emitting diodes with ultra high brightness. *Chin. Phys. B* **2013**, *22*, 077303. [[CrossRef](#)]
161. Liu, B.; Xu, M.; Tao, H.; Su, Y.J.; Gao, D.Y.; Zou, J.H.; Lan, L.F.; Peng, J.B. The effect of spacer in hybrid white organic light emitting diodes. *Chin. Sci. Bull.* **2014**, *59*, 3090–3097. [[CrossRef](#)]

162. Liu, B.; Xu, M.; Wang, L.; Tao, H.; Su, Y.; Gao, D.; Zou, J.; Lan, L.; Peng, J. Comprehensive Study on the Electron Transport Layer in Blue Fluorescent Organic Light-Emitting Diodes. *ECS J. Solid State Sci. Technol.* **2015**, *2*, R258–R261. [[CrossRef](#)]
163. Sun, H.D.; Guo, Q.X.; Yang, D.Z.; Chen, Y.H.; Chen, J.S.; Ma, D.G. High Efficiency Tandem Organic Light Emitting Diode Using an Organic Heterojunction as the Charge Generation Layer: An Investigation into the Charge Generation Model and Device Performance. *ACS Photonics* **2015**, *2*, 271–279. [[CrossRef](#)]
164. Ding, L.; Sun, Y.Q.; Chen, H.; Zu, F.S.; Wang, Z.K.; Liao, L.S. A novel intermediate connector with improved charge generation and separation for large-area tandem white organic lighting devices. *J. Mater. Chem. C* **2014**, *2*, 10403–10408. [[CrossRef](#)]
165. Chang, C.C.; Chen, J.F.; Hwang, S.W.; Chen, C.H. Highly efficient white organic electroluminescent devices based on tandem architecture. *Appl. Phys. Lett.* **2005**, *87*, 253501. [[CrossRef](#)]
166. Yook, K.S.; Jeon, S.O.; Min, S.Y.; Lee, J.Y.; Yang, H.J.; Noh, T.; Kang, S.K.; Lee, T.W. Highly Efficient p-i-n and Tandem Organic Light-Emitting Devices Using an Air-Stable and Low-Temperature-Evaporable Metal Azide as an n-Dopant. *Adv. Funct. Mater.* **2010**, *20*, 1797–1802. [[CrossRef](#)]
167. Liu, B.; Wang, L.; Tao, H.; Xu, M.; Zou, J.; Ning, H.; Peng, J.; Cao, Y. Doping-Free Tandem White Organic Light-Emitting Diodes. *Sci. Bull.* **2017**, *62*, 1193–1200. [[CrossRef](#)]
168. Wu, Z.; Yu, L.; Zhao, F.; Qiao, X.; Chen, J.; Ni, F.; Yang, C.; Ahamad, T.; Alshehri, S.M.; Ma, D. Precise Exciton Allocation for Highly Efficient White Organic Light-Emitting Diodes with Low Efficiency Roll-Off Based on Blue Thermally Activated Delayed Fluorescent Exciplex Emission. *Adv. Opt. Mater.* **2017**, *5*, 1700415. [[CrossRef](#)]
169. Sun, N.; Wang, Q.; Zhao, Y.B.; Yang, D.Z.; Zhao, F.C.; Chen, J.S.; Ma, D.G. A hybrid white organic light-emitting diode with above 20% external quantum efficiency and extremely low efficiency roll-off. *J. Mater. Chem. C* **2014**, *2*, 7494–7504. [[CrossRef](#)]
170. Liu, B.; Zou, J.H.; Su, Y.J.; Gao, D.Y.; Lan, L.F.; Tao, H.; Peng, J.B. Hybrid white organic light emitting diodes with low efficiency roll-off, stable color and extreme brightness. *J. Lumin.* **2014**, *151*, 161–164. [[CrossRef](#)]
171. Luo, D.; Xiao, Y.; Hao, M.M.; Zhao, Y.; Yang, Y.B.; Gao, Y.; Liu, B.Q. Doping-free white organic light-emitting diodes without blue molecular emitter: An unexplored approach to achieve high performance via exciplex emission. *Appl. Phys. Lett.* **2017**, *110*, 061105. [[CrossRef](#)]
172. Huang, W.Y.; Chen, Z.W.; You, H.W.; Fan, F.C.; Chen, H.F.; Wong, K.T. Efficient carrier- and exciton-confining device structure that enhances blue PhOLED efficiency and reduces efficiency roll-off. *Org. Electron.* **2011**, *12*, 575–581. [[CrossRef](#)]
173. Duan, L.; Zhang, D.Q.; Wu, K.W.; Huang, X.Q.; Wang, L.D.; Qiu, Y. Controlling the Recombination Zone of White Organic Light-Emitting Diodes with Extremely Long Lifetimes. *Adv. Funct. Mater.* **2011**, *21*, 3540–3545. [[CrossRef](#)]
174. Liu, B.; Wang, L.; Xu, M.; Tao, H.; Zou, J.H.; Gao, D.Y.; Lan, L.F.; Ning, H.; Peng, J.B.; Cao, Y. Efficient Hybrid White Organic Light-emitting Diodes with Extremely Long Lifetime: The Effect of n-type Interlayer. *Sci. Rep.* **2014**, *4*, 7198. [[CrossRef](#)] [[PubMed](#)]

